

MARKOV-CHAIN MODULATED IMPLIED LIQUIDITY: MODELING AND  
ESTIMATION

A THESIS SUBMITTED TO  
THE GRADUATE SCHOOL OF APPLIED MATHEMATICS  
OF  
MIDDLE EAST TECHNICAL UNIVERSITY

BY

ÇİĞDEM YERLİ

IN PARTIAL FULFILLMENT OF THE REQUIREMENTS  
FOR  
THE DEGREE OF DOCTOR OF PHILOSOPHY  
IN  
FINANCIAL MATHEMATICS

MAY 2023



Approval of the thesis:

**MARKOV-CHAIN MODULATED IMPLIED LIQUIDITY: MODELING AND ESTIMATION**

submitted by **ÇİĞDEM YERLİ** in partial fulfillment of the requirements for the degree of **Doctor of Philosophy in Financial Mathematics Department, Middle East Technical University** by,

Prof. Dr. Sevtap Kestel  
Dean, Graduate School of **Applied Mathematics**

\_\_\_\_\_

Prof. Dr. Sevtap Kestel  
Head of Department, **Financial Mathematics**

\_\_\_\_\_

Prof. Dr. Sevtap Kestel  
Supervisor, **Department of Actuarial Sciences, METU**

\_\_\_\_\_

Assoc. Prof. Dr. Zehra Ekşi-Altay  
Co-supervisor, **Institute for Statistics and Mathematics, WU**

\_\_\_\_\_

**Examining Committee Members:**

Prof. Dr. Serkan Eryılmaz  
Department of Industrial Engineering, Atılım University

\_\_\_\_\_

Prof. Dr. Sevtap Kestel  
Department of Actuarial Sciences, METU

\_\_\_\_\_

Prof. Dr. Ali Devin Sezer  
Department of Financial Mathematics, METU

\_\_\_\_\_

Prof. Dr. Ömür Uğur  
Department of Scientific Computing, METU

\_\_\_\_\_

Assoc. Prof. Dr. Özge Sezgin Alp  
Department of Accounting and Finance Management,  
Başkent University

\_\_\_\_\_

**Date:**

\_\_\_\_\_



**I hereby declare that all information in this document has been obtained and presented in accordance with academic rules and ethical conduct. I also declare that, as required by these rules and conduct, I have fully cited and referenced all material and results that are not original to this work.**

Name, Last Name: ÇİĞDEM YERLİ

Signature :



# ABSTRACT

## MARKOV-CHAIN MODULATED IMPLIED LIQUIDITY: MODELING AND ESTIMATION

Yerli, Çiğdem

Ph.D., Department of Financial Mathematics

Supervisor : Prof. Dr. Sevtap Kestel

Co-Supervisor : Assoc. Prof. Dr. Zehra Ekşi-Altay

May 2023, 86 pages

This thesis presents a methodology for modeling the implied liquidity which is introduced through the Conic Finance theory, and considered a proxy for the market liquidity level. We propose a partial information setting in which the dynamics of implied liquidity, representing the noisy information on the unobserved true market liquidity, follow a continuous-time Markov-chain modulated exponential Ornstein-Uhlenbeck process. Model inference requires the filtering of the unobserved states of the true market liquidity, as well as the estimation of the unknown model parameters. We address the inference problem by the EM algorithm. The expectation step of the algorithm requires the derivation of finite dimensional filters for the quantities present in the likelihood function. To this end, we first review the existing EM algorithm for the OU process and provide detailed proofs. The application of the algorithm in practice needs discretizing the resulting filters. In order to avoid numerical issues and make the algorithm to function, we introduce filters that have a continuous dependence on the observations. The corresponding filters are known as robust filters. Instead of directly discretizing continuous time filters, we discretize the robust filters that help us to work under the discrete time setting and also enable us to obtain the variance estimate of the model within the EM algorithm. We evaluate the performance of the algorithm and compare it to existing alternatives in the literature using an extensive simulation study. The performance evaluation is based on the sensitivity

to changes in step size, drift, and volatility parameters. This step is crucial for refining the methods and establishing a connection between theory and practice. Once the algorithm is tested with simulated data, we apply the proposed model to real world data. The data set is comprised of implied market liquidity series retrieved from the S&P 500 option data covering the period from January 2002 to August 2022. Our application results show that three liquidity regimes can describe the market liquidity level: high, intermediate and low. The estimation results confirm the effect of the overall economic environment on the market liquidity.

**Keywords:** Expectation maximization (EM) algorithm, hidden Markov models, Ornstein-Uhlenbeck processes, robust filters, implied liquidity



# ÖZ

## MARKOV ZİNCİRİ MODÜLASYONLU ZİMNİ LİKİDİTE: MODELLEME VE TAHMİN

Yerli, Çiğdem

Doktora, Finansal Matematik Bölümü

Tez Yöneticisi : Prof. Dr. Sevtap Kestel

Ortak Tez Yöneticisi : Doç. Dr. Zehra Ekşi-Altay

Mayıs 2023, 86 sayfa

Bu tez, Konik Finans teorisi aracılığıyla tanıtılan ve piyasa likidite düzeyi için bir temsil olarak kabul edilen zımnî likiditeyi modellemek için bir metodoloji sunmaktadır. Gözlemlenemeyen gerçek piyasa likiditesine ilişkin gürültülü bilgileri temsil eden zımnî likidite dinamiklerinin, sürekli zamanlı Markov zinciri modülasyonlu üstel Ornstein-Uhlenbeck sürecini takip ettiği, bilginin kısmi olduğu bir çerçeveye önerilmektedir. Model çıkarımı, gerçek piyasa likiditesinin gözlemlenmemiş durumlarının filtrelenmesini ve ayrıca bilinmeyen model parametrelerinin tahmin edilmesini gerektirir. Çıkarım problemi EM algoritması ile ele alınmaktadır. Algoritmanın beklenti adımı, olabilirlik fonksiyonunda bulunan nicelikler için sonlu boyutlu filtrelerin türetilmesini gerektirir. Bu amaçla, öncelikle OU süreci için mevcut EM algoritmasını incelenerek ayrıntılı ispatları sunulmaktadır. Algoritmanın pratik uygulaması sırasında, ortaya çıkan filtrelerin ayrıklaştırılması gerekmektedir. Sayısal sorunlardan kaçınmak ve algoritmanın çalışmasını sağlamak için gözlemlere sürekli bağlı olan filtreleri tanıtılmaktadır. Karşılık gelen filtreler sağlam (robust) filtreler olarak bilinir. Sürekli zaman filtrelerini doğrudan ayrıklaştırmak yerine, ayrık zaman ayarı altında çalışmamıza yardımcı olan ve aynı zamanda modelin varyans tahminini EM algoritması içinde elde etmemizi sağlayan sağlam filtreleri ayrıklaştırılmaktadır. Kapsamlı bir simülasyon çalışması kullanarak algoritmanın performansını değerlendirilmekte ve literatürdeki mevcut alternatiflerle karşılaştırılmaktadır. Performans değerlendir-

mesi, adım boyutu, sapma ve oynaklık parametrelerindeki deęişikliklere olan duyarlılığı temel alır. Bu adım, yöntemleri geliştirmek ve teori ile pratik arasında bir bağlantı kurmak için çok önemlidir. Algoritma simüle edilmiş verilerle test edildikten sonra, önerdiğimiz modeli gerçek verilere uygulanmaktadır. Veri seti, 1 Ocak 2002 - 1 Ağustos 2022 dönemini kapsayan S&P 500 opsiyon verilerinden alınan zımni piyasa likidite serilerinden oluşmaktadır. Uygulama sonuçları, üç likidite rejiminin piyasa likidite seviyesini tanımlayabildiğini göstermektedir: yüksek, orta ve düşük. Tahmin sonuçları, genel ekonomik ortamın piyasa likiditesi üzerindeki etkisini doğrulamaktadır.

Anahtar Kelimeler: Beklenti maksimizasyonu (EM) algoritması, saklı Markov modelleri, Ornstein-Uhlenbeck süreci, sağlam filtreler, zımni likidite

*To my family*



## ACKNOWLEDGMENTS

I would like to express my sincere gratitude and appreciation to my thesis supervisor, Prof. Dr. A. Sevtap Kestel, for her exceptional guidance, unwavering support, and valuable insights throughout the entire process of developing and preparing this thesis. Her patience, enthusiasm, and willingness to dedicate time and share her expertise have been invaluable. Her mentorship has illuminated my path.

I would like to express my heartfelt appreciation to my co-supervisor, Assoc. Prof. Dr. Zehra Eksi-Altay, for her willingness to collaborate with me and her invaluable contribution to expanding the research topic. I am truly grateful for her patience, kindness, enthusiastic encouragement and valuable advices throughout the research process. Her guidance has been instrumental in shaping my understanding and approach. I am fortunate to have had the opportunity to work with her and I sincerely thank her for her support and expertise.

I also would like to thank my thesis examining committee members, Prof. Dr. Serkan Eryılmaz, Prof. Dr. Ali Devin Sezer, Prof. Dr. Ömür Uğur and Assoc. Prof. Dr. Özge Sezgin Alp for the time and thoughts that they devoted to this work.

I thank the faculty and staff of the Institute of Applied Mathematics, METU for the support they provided from the beginning till end of my PhD journey. Moreover I express my appreciation to TUBITAK (The Scientific and Technological Research Council of Turkey) which provided financial support through projects 2211-B and 2214-A. Additionally, I thank the faculty and staff of the Institute for Statistics and Mathematics, WU, Austria, for their warm hospitality during my research visit. I am deeply grateful to all these institutions and individuals for their contributions and support, which have played a significant role in shaping my academic journey.

I thank to my friends Aysen, Aysegul and Gaye for their support during my research. I am fortunate to have such amazing friends by my side. I also extend my special thanks to my dear friend Ismail for his endless support and love. His unwavering belief in me and his constant encouragement have been a source of strength and inspiration. I am truly grateful for his presence in my life.

Last but not least, I would like to convey my profound appreciation to my beloved family for their unwavering support. To my dear parents, Yeter and Ali, you deserve the utmost admiration and gratitude for the countless sacrifices you have made for your children. Your love and encouragement have been the foundation of my success. I also want to express my thanks to my siblings, Nuran, Sinem, and Seyit Can, for the

cherished memories we shared during our childhood. These memories have provided me with immense inner strength throughout my studies. Without the presence and support of my incredible family, this journey would not have been possible. I am forever grateful for your love and support.

# TABLE OF CONTENTS

ABSTRACT . . . . .	vii
ÖZ . . . . .	ix
ACKNOWLEDGMENTS . . . . .	xiii
TABLE OF CONTENTS . . . . .	xv
LIST OF TABLES . . . . .	xix
LIST OF FIGURES . . . . .	xx
LIST OF ABBREVIATIONS . . . . .	xxii
CHAPTERS	
1 INTRODUCTION . . . . .	1
1.1 Introduction . . . . .	1
1.2 Motivation and contribution . . . . .	3
1.3 Structure of the thesis . . . . .	6
2 REVIEW OF MARKET LIQUIDITY MEASURES . . . . .	9
2.1 Introduction . . . . .	9
2.1.1 Volume based liquidity measures . . . . .	10
2.1.2 Price impact based liquidity measures . . . . .	12

	2.1.3	Transaction cost based liquidity measures . . . . .	14
3		PRELIMINARIES . . . . .	19
	3.1	Conic Finance Theory . . . . .	19
	3.2	The Ornstein-Uhlenbeck Process . . . . .	24
	3.2.1	Exponential Ornstein-Uhlenbeck Process . . . . .	26
4		MODEL AND ESTIMATION . . . . .	29
	4.1	Model setting and notation . . . . .	29
	4.1.1	EM algorithm for the current setting . . . . .	32
	4.2	Filtering . . . . .	36
	4.2.1	Continuous time filters . . . . .	36
	4.2.2	Robust Filters . . . . .	44
	4.2.2.1	Discrete time filters . . . . .	47
	4.2.2.2	Variance Estimation . . . . .	50
5		SIMULATION STUDY . . . . .	53
	5.1	Simulation . . . . .	53
	5.1.1	How does $\Delta$ affect the performance of the EM algorithm? . . . . .	56
	5.1.2	How does drift (relative to noise variance) affect the performance of the EM algorithm? . . . . .	58
	5.1.3	How does the noise variance affect the performance of the EM algorithm? . . . . .	59
6		DATA APPLICATION . . . . .	63
	6.1	Data . . . . .	63



6.2	In sample results . . . . .	64
6.2.1	Model selection and error analysis . . . . .	68
6.3	Out of sample results . . . . .	71
7	CONCLUSION . . . . .	75
	REFERENCES . . . . .	77
APPENDICES		
A	APPENDICES . . . . .	83
A.1	Possible states in the data . . . . .	83
A.2	Results of static out of sample test . . . . .	83
	CURRICULUM VITAE . . . . .	85



## LIST OF TABLES

Table 3.1	Parameters used in simulation . . . . .	26
Table 5.1	Parameters used in the algorithm . . . . .	55
Table 6.1	Initial parameters used in empirical analysis . . . . .	65
Table 6.2	The initial values of the generator matrix . . . . .	65
Table 6.3	Parameter estimates . . . . .	66
Table 6.4	Results of error analysis - in sample results . . . . .	70
Table 6.5	Results of error analysis - out of sample results . . . . .	73

## LIST OF FIGURES

Figure 2.1	Dimensions of liquidity [26] . . . . .	10
Figure 3.1	Simulated path - OU process . . . . .	26
Figure 3.2	Simulated path - Exponential OU process . . . . .	27
Figure 5.1	Markov chain and noisy observation process . . . . .	56
Figure 5.2	EM estimates vs. true chain, $\Delta = 1/80$ . . . . .	56
Figure 5.3	Evolution of parameter estimates for $A, g$ and $\kappa$ , $\Delta = 1/80$ . . . . .	57
Figure 5.4	EM estimates vs. true chain, $\Delta = 1/250$ . . . . .	57
Figure 5.5	Evolution of parameter estimates for $A, g$ and $\kappa$ , $\Delta = 1/250$ . . . . .	58
Figure 5.6	EM estimates vs. true chain, $g = [-1 \ 0.2 \ 1]$ . . . . .	59
Figure 5.7	Evolution of parameter estimates for $A, g$ and $\kappa$ , $g = [-1 \ 0.2 \ 1]$ . . . . .	60
Figure 5.8	EM estimates vs. true chain . . . . .	61
Figure 5.9	Evolution of parameter estimates for $A, g$ and $\kappa$ . . . . .	61
Figure 6.1	Log of implied liquidity (basis points) . . . . .	64
Figure 6.2	Filtered states: 2-state MC (top) and 3-state MC (bottom) . . . . .	65
Figure 6.3	Evolution of parameter estimates for $A, g, \varsigma$ and $\kappa$ Top: 2-state MC and bottom: 3-state MC . . . . .	66
Figure 6.4	Fitted value vs real data: 2-state MC (top) and 3-state MC (bottom) . . . . .	70
Figure 6.5	Evolution of parameter estimates for $A, g, \varsigma$ and $\kappa$ 2-state MC (top) and 3-state MC (bottom) . . . . .	71
Figure 6.6	1-day ahead prediction: 2-state MC (top) and 3-state MC (bottom) . . . . .	72
Figure 6.7	Interval forecast: 2-state MC (top) and 3-state MC (bottom) . . . . .	72

Figure A.1 Possible states in the data . . . . .	83
Figure A.2 Evolution of parameter estimates for $A$ , $g$ , $\varsigma$ and $\kappa$ 2-state MC (top) and 3-state MC (bottom) . . . . .	83
Figure A.3 1-day ahead prediction: 2-state MC (top) and 3-state MC (bottom) .	84
Figure A.4 Interval forecast: 2-state MC (top) and 3-state MC (bottom) . . . .	84

## LIST OF ABBREVIATIONS

AIC	Akaike information criteria
BIC	Bayesian information criteria
CEV	Constant elasticity of variance
CIR	Cox–Ingersoll–Ross
EM	Expectation-Maximization
ES	Effective spread
E-step	Expectation step
Fed	Federal reserve
HMM	Hidden Markov model
ILR	Illiquidity ratio
LR	Liquidity ratio
MAE	Mean absolute error
MAPE	Mean absolute percentage error
MC	Markov chain
MI	Martin Index
MLE	Maximum likelihood estimation
M-step	Maximization step
ODE	Ordinary differential equation
OU	Ornstein-Uhlenbeck
SDE	Stochastic differential equation
RAE	Relative absolute error
RMSE	Root mean squared error
RS	Realized spread
QE	Quantitative easing
QS	Quoted spread
TSE	Total squared error

# CHAPTER 1

## INTRODUCTION

### 1.1 Introduction

Market liquidity has crucial importance in the smooth functioning of financial markets. The liquidity, or lack thereof, in business sectors can greatly influence the financial system and overall economy, disrupting their normal operations. The Russian financial crisis and the Long-Term Capital Management crash in 1998 are examples of how a minor disruption in liquidity can have a significant and unanticipated impact on the market. More recently, the financial crisis of 2008 highlighted the importance of liquidity in financial markets, once more bringing the issue to the forefront.

There is no single, universally accepted definition of liquidity; instead, different perspectives and interpretations exist. Various economists and financial experts have offered different perspectives on what constitutes liquidity and how it should be measured. According to [43], any asset that can be bought or sold in large quantities quickly with minimal effect on its price is considered liquid in the market. Demsetz (1968) [25] defines market liquidity as the price adjustments that market actors must make to execute a trade. This definition suggests that in liquid markets, participants can execute trades without experiencing significant transaction costs or price concessions. Shen and Starr (2002) [56] define liquidity in financial markets as the capacity to efficiently handle the influx and outflow of orders for buying and selling, while [31] defines a market as liquid if trades can be carried out without incurring any transaction costs, drawing on definitions from [30]. In [15], liquidity refers to the ease and cost efficiency of executing large volume trades for a given asset. Overall, liquidity

is related to a market's ability to handle large transaction volumes without causing significant price movements or transaction costs in a short time period.

The lack of a precise definition of market liquidity makes measuring liquidity complex task. In the literature, the liquidity measures are categorized under three main groups: volume based, transaction cost based, and price impact based [54], which are essential in defining liquidity and can be measured through various dimensions. Oesterhelweg and Schiereck (1993) [49] discuss the dimensions of liquidity, and [54] identify five dimensions: breadth, depth, immediacy, resilience, and tightness. Breadth refers to the amount and size of orders around equilibrium prices, while depth concerns the number of orders at those prices. Immediacy pertains to how quickly orders can be executed, while resilience refers to the market's ability to bounce back from unforeseen events. Tightness is associated with the level of transaction costs. The concept of market liquidity encompasses many dimensions, making it challenging to capture with a single statistic. Instead, there are various methods and metrics to measure liquidity, each with advantages and limitations. Bid-ask spread as a transaction cost based approach is the most commonly used indicator to evaluate the level of market liquidity (see [24], [57], [22], and [4]). Despite its usefulness, many models based on bid-ask spreads do not fully account for the observed magnitude of spreads in financial markets. This was particularly evident after the 2008 financial crisis, during which bid-ask spreads for many assets remained consistently high, surpassing what could be explained by transaction costs alone [50]. Furthermore, bid-ask spread can fluctuate in response to volatility or changes in the spot price of an asset, regardless of whether the underlying liquidity of the asset has actually changed [20].

Another approach related with bid and ask prices is based on the theory of Conic Finance, and is first introduced by [12] and is further developed by [47]. The foundation of this approach is that there are two prices in the market: ask price to buy from the market and bid price to sell to the market. In this perspective, as a counterparty, the market executes all eligible trades, determined by acceptability indices derived from Artzner's theory of coherent risk measures [3]. In the Conic Finance theory, market liquidity level is modeled through a market stress parameter that matches the market bid and ask prices with the theoretical bid and ask prices calculated based on the acceptability indices assigned by the market. These indices are derived from the



deviation of the risk-neutral pricing measure. Corcuera et al. (2012) [20] introduce an implied liquidity parameter as a unitless quantity to facilitate liquidity comparisons across different assets and markets. Calculating it for different strikes and maturities results in implied liquidity surfaces. Then, the authors analyzed its behavior over time, specifically for ATM calls on US indices. It is observed that during the 2008 financial crisis, the implied liquidity parameter increased, indicating a significant reduction in liquidity in major vanilla markets. It is also noticed that implied liquidity is mean-reverting and resembles stochastic volatility in behavior. In this regard, [1] model the implied liquidity with different stochastic models: CIR, Vasicek, and CEV models. They assess the model sensitivity of stochastic implied liquidity and examine the effect of the financial crisis on implied liquidity by considering the pre- and post-crisis periods. The authors suggested a stochastic, regime switching, mean-reverting process for modeling liquidity. Leippold and Schärer (2017) [44] develop a stochastic liquidity model, extending an existing model by [47] that assumes constant liquidity over time. Their model enables the replication of the term and skew structures of bid-ask spreads commonly observed in options markets. They provide a method for implementing the stochastic liquidity model using multidimensional binomial trees and calibrate it to call and put options on the S&P 500. The stochastic liquidity modeling approach is believed to be highly valuable in structured asset pricing, hedging activities, and risk management.

## **1.2 Motivation and contribution**

Albrecher et al. (2013) [1] puts forward that their analysis of implied liquidity may lead to the use of a stochastic, regime-switching mean-reverting process for modeling liquidity. Based on this observation, we fit a Markov modulated mean-reverting model to the observed implied liquidity series. Note that, the objective of this thesis is not to extend the standard Conic Finance Theory to the stochastic/dynamic setting. Following [1], we consider our efforts as a first step towards stochastic liquidity modeling.

This research proposes a new method for modeling the implied liquidity using a continuous time Markov chain modulated exponential Ornstein-Uhlenbeck (OU) process

under partial information setting. The estimation methodology is based on non-linear filtering tools and the EM algorithm. The dynamics of market liquidity is examined and economic motivations are provided through the application of the model to real market data. Elliott et al. (1999) [28] introduces the filtering and parameter estimation for the Markov chain modulated OU process. Our novel contribution is that, for the same setting, we provide an EM algorithm methodology with robust filtering and discretization in the sense of [42]. Robust filters are required to avoid numerical issues that may arise in applications with discrete observations. That also allows us to estimate the unknown noise variance within the algorithm.

The motivation is to use a continuous time hidden Markov chain modulated exponential OU process is explained below.

It is common to observe structural regime changes in both macroeconomic environment and financial markets. Market liquidity, naturally, is affected by economic regimes like quantitative easing and tightening, or financial market regimes like bullish and bearish conditions. Moreover, market liquidity has a "self-stabilizing effect" in either good or poor economic conditions as noted by [8, 7]. As mentioned previously, [20] and [1] observed the mean-reverting behavior of the implied liquidity.

We consider a partial information setting because hidden variables, such as expectations, information, risk aversion, and beliefs, are prevalent in economies, making it difficult to fully observe the true state of the underlying market liquidity level. Knowing the true state is crucial for decision making in the economy. There are several ways to address this problem. One approach is to focus on measurable variables, but this can lead to high systematic errors and high variance in forecasts, as the effects of changes in economic states on observable variables are ignored. Another approach is to estimate latent variables, for which statistical methods such as principal component analysis and factor analysis are commonly used. Hidden Markov model (HMM) is another approach to uncover hidden states from observable market data. Even if the regime switches are assumed to represent economic decisions that are observable to market agents, the impact of these decisions may come earlier or later than the actual time the decision is made. Thus, these hidden changes can be captured by a HMM.

Finally, the proposed model ensures the non-negativity of the implied liquidity whose construction requires the non-negative results as the ask price is always higher than the bid price. In the extreme case, when the bid price and ask price are equal, the implied liquidity is equal to zero, and the two price model becomes a one price model.

We suggest a hidden Markov chain modulated exponential OU process to capture the positivity, mean reversion and regime switching behavior on observed implied liquidity series.

There are several studies in the literature that use the hidden Markov model approach to examine market liquidity regimes. For example, [32] study the commonalities in market liquidity with the goal of identifying broad patterns that can be used to monitor systemwide liquidity conditions. They employ 33 time series daily data covering four asset classes, namely equities, corporate bonds, oil futures and volatility index futures over the period over the period from 2004 to 2014. Then they apply Bayesian hidden Markov chain models to capture the latent structure of each series and assess the liquidity dynamics at the systemwide level. This approach helps to normalize local liquidity conditions, making them directly comparable across markets and order flow conditions, and allows for the identification of sudden changes in price impact that are driven by underlying liquidity states. They conclude that there are three liquidity regimes: low, intermediate, and high. Tenyakov et al. (2016) [58] focus on modeling the risk arising from market and funding liquidity by examining the joint dynamics of three monthly time series: the Treasury-Eurodollar spread, the VIX, and a metric derived from the S&P 500 spread over the period from 1998 to 2013. To capture liquidity levels, the authors use a discrete time multivariate HMM OU model process expressed in matrix representation and conclude that 2-state model is sufficient. Chen et al. (2020) [11] examine the relationship between funding liquidity and market liquidity and how it varies over time. The researchers use a discrete time Markov regime switching model to analyze the dynamic patterns of financial time series that is a comprehensive US TRACE data set from 2004 to 2013. The study concludes that funding liquidity and corporate bond market liquidity are interconnected, their influence on each other is heavily dependent on the economic regime changes, and two regimes are sufficient to explain the funding liquidity and market liquidity and understand their relationship. Finally, Gu et al. (2021) [38] propose a hybrid mul-

tivariate discrete time HMM approach to capture the regime switching dynamics of four financial market indicators that are deemed to drive the main characteristics of liquidity risk: Treasury-Euro Dollar rate spread, US dollar index, volatility index and S&P 500 metric over the period from 1998 to 2018. The approach involves an on-line system that processes observed indicators and interfaces with an advanced alert mechanism to give appropriate measures. Two stochastic models, namely geometric Brownian motion and OU process with HMM-modulated parameters are integrated to capture the evolutions of the four time series and show the sufficiency of two regimes in explaining the dynamics.

Our aim is to evaluate the market liquidity through the use of implied liquidity as a proxy for the market liquidity level. Following the idea by [1], we model the implied liquidity with a continuous time hidden Markov modulated OU process. We assume that the implied liquidity series provide noisy information on the true market liquidity level, thus we cannot observe the true liquidity level directly and can only observe the implied liquidity series. To estimate the unknown parameters in the model, we use the EM algorithm. The continuous time filters that are required in the expectation step (E-step) of the algorithm are originally derived in [28]. We introduce the corresponding robust filters of continuous time filters in the sense of [42]. This is a discrete time setting which provides an explicit approximation of the continuous time filters. Moreover, working with discretized robust filters help us to introduce the variance estimate of the model, which is not possible to estimate in the continuous time model setting. Our data application results show that three liquidity regimes can describe the market liquidity level reasonably well: high, intermediate and low. Thus, with the help of our proposed model, we can provide guidance to perspectives of any participant in the economy such as policy makers, investors who aim to detect, evaluate and predict the unstable periods in the financial system.

### **1.3 Structure of the thesis**

Chapter 2 gives the review of market liquidity measures with related literature. The measures are categorized into three main groups: volume based, price impact based and transaction cost based. Bid-ask spread related measures are generally included

in the transaction cost based measures although they can be used in other categories. Implied liquidity, obtained from Conic Finance Theory, is also one of the bid-ask spread related approaches to evaluate the market liquidity. Thus, we also give brief information about the implied liquidity.

In Chapter 3, we briefly give mathematical background related with the theory used in this work. In details, we review the Conic Finance Theory to explain the basics of the implied liquidity since we use the implied liquidity as a proxy for the market liquidity level. Then, we recall OU process and its exponential version.

In Chapter 4, we introduce our approach to estimate the unknown parameters in the Markov chain modulated OU model by using the EM algorithm. First, we give the notation and setting required to introduce our model. Specifically, we assume that true market liquidity level is naturally dependent on the macroeconomic environment and we consider a continuous time Markov modulated model under the partial information setting since true market liquidity states cannot be observed directly, we only observe the implied liquidity series. To make a statistical inference for the hidden Markov model, we use the Expectation Maximization (EM) algorithm. Accordingly, we review the EM algorithm for Markov chain modulated OU process given in [28] at which the proofs are not provided in [28]. For the thesis to be self contained, we provide them in detail. The implementation of the algorithm needs the filters that depend on the observations continuously. These filters are known as robust filters [17, 42]. Thus, we derive the robust filters for our framework by following the idea introduced in [17, 42]. This approach provides a discrete time setting which provides an explicit approximation of the continuous time filters. Finally, working with discretized robust filters makes it possible to introduce the variance estimate of the model, which is not possible to estimate in the continuous time model setting.

In Chapter 5, the performance of algorithms is evaluated and compared. The estimation methodology of the algorithms use two types of filters: discretized robust filters and discretized continuous time filters. For the simulation study, the continuous time filters are discretized using both Euler and Milstein approaches. As for robust versions, introduced discretized robust filters are used. The performance of the algorithms is evaluated based on their sensitivity to changes in step size, drift,

and volatility parameters. This examination is essential for refining the methods and establishing a connection between theoretical concepts and their practical implementation.

In Chapter 6, we provide a real data application under a proposed model setting. This part aims to evaluate the market liquidity through the use of implied liquidity. First, we describe the data and explain how to derive it. After applying our proposed model to the data, we evaluate the results based on in sample and out of sample results. Specifically, we decide the number of states using Akaike information criteria (AIC) and Bayesian information criteria (BIC) based on in sample results. In out of sample testing, we evaluate the performance of the proposed model according to point forecast and interval forecast results.

Finally, Chapter 7 provides a summary of the main findings and a discussion of potential future studies.

## CHAPTER 2

### REVIEW OF MARKET LIQUIDITY MEASURES

#### 2.1 Introduction

There is no single, universally accepted definition of liquidity, and different perspectives and interpretations exist. As mentioned previously, liquidity is related to a market's ability to handle large transaction volumes without causing significant price movements or transaction costs in a short time period. Thus, the definitions in the literature can be collected under four aspects [34]: time, tightness, depth and resiliency.

Time dimension is related with the execution of a trade quickly at the current market price. The immediacy of the trade, or the speed at which trades of a certain size can be executed with given costs, can be calculated by the waiting time between trades or or the quantity of trades done in a given period of time. The tightness of the market, or the ability to purchase and sell a security at nearly the same price at the same time, can be measured by the difference between the best bid and ask quotes. This aspect is often viewed as a representation of transaction costs. Depth dimension refers to the ability to exchange a large amount of a security without significantly impacting the market price. A market is considered deep if there are a large number of orders at different prices, so that executing a trade does not significantly change the quoted price. Resiliency dimension is related with the capability to trade a large volume of a security without significantly affecting its quoted price. A market is considered to be resilient if it can handle changes in order volume and respond to new information or price changes without causing significant price fluctuations. It is a measure of the

price-volume elasticity of an asset, and reflects the ability to maintain stability in the face of change. The four dimensions of the liquidity is presented in the Figure 2.1.

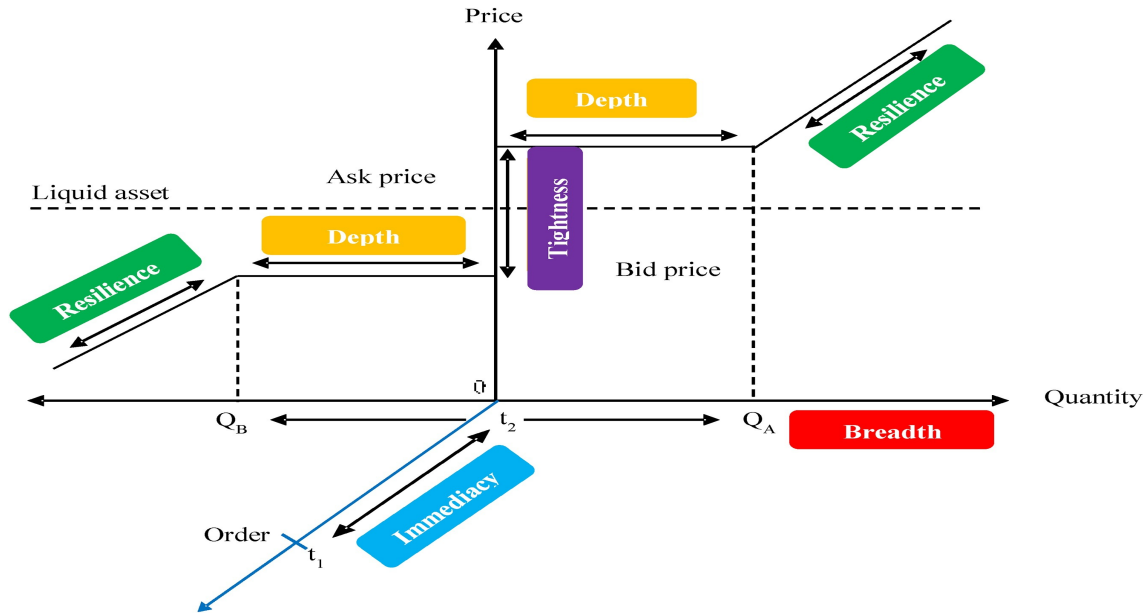


Figure 2.1: Dimensions of liquidity [26]

According to [2], market liquidity is a complex concept that cannot be fully represented by a single measure. As a result, various measures have been developed to capture different aspects of liquidity, leading to various approaches for categorizing liquidity measures. [35] categorize liquidity measures into three categories: volume based, price impact based, and transaction cost based. The volume based measures evaluate the relationship between price and quantity and the degree of a transaction’s price impact. The second measures liquidity based on price behavior. The third covers bid-ask spread and its variants and measures liquidity in terms of transaction costs.

### 2.1.1 Volume based liquidity measures

Volume based liquidity measures determine the liquidity of securities by the amount of transactions. A security is considered liquid if it has a high volume of transactions, meaning that there is a large demand for the security and many trades take their place. Conversely, a security is considered illiquid if it has a low volume of transactions.

Volume based measures of liquidity, as explained by [54], assess the characteristics of market breadth and depth through the number of transactions. These measures are



beneficial in gauging the extent of market activity, with both a high number and large volume of orders being a good indication. Dealers can easily execute orders without assuming any significant inventory positions if there is an abundance of orders from both buyers and sellers, making volume based measures a popular way to assess liquidity. Trading volume and turnover ratio are the metrics in this area that are most frequently utilized. Trading volume is a simple and direct way of measuring liquidity. It represents the total number of shares that have been traded in a given period by market makers in their buying and selling activities. It is typically expressed as dollar trading volume  $Vol$ , which is calculated as follows:

$$Vol_i = \sum_{j=1}^N P_{i,n}^j \times V_{i,n}^j$$

where, for a stock  $i$ , a time period  $n$  and transaction  $j$ ,  $P_{i,n}^j$  is stock price, and  $V_{i,n}^j$  is quantity of the stock.

It is widely used and considered to be an indicator of liquidity, with high trading volume implying low security illiquidity. However, trading volume has a limitation in that it can lead to double counting.

Another volume based liquidity metric is the turnover ratio, which is derived by dividing the number of traded shares by the total number of shares outstanding. The formula for this ratio is as follows:

$$Turnover = (1/N) \sum_{n=1}^N \frac{V_{i,n}}{Sout_{i,n}}$$

where, for a stock  $i$ , a time period  $n$ ,  $Turnover$  is the turnover ratio,  $N$  represents the number of trading days,  $V_{i,n}$  represents the daily number of shares traded, and  $Sout_{i,n}$  represents the daily number of outstanding shares.

Easley and O'Hara (1992) [27] find that trading frequency conveys important market information and has a significant impact on liquidity. As turnover gives information about trading frequency, it can be used as an indicator of stock liquidity. Additionally, turnover ratio is often seen as a superior liquidity measure compared to trading volume, as it takes into account the market capitalization of stocks [35]. The availability of monthly and daily data for turnover ratio is an advantage and enables the capture of liquidity of stocks over a long period of time. For these reasons, turnover ratio is

frequently used as a proxy for liquidity in studies, e.g., [14] and [48].

Despite its advantages, using volume based measures as liquidity indicators still has limitations. According to [35], these measures fail to capture how prices change in response to sudden orders. They are only effective as a beginning point in the analytical process because they are not derived from theoretical models that describe market maker behavior and solely capture historical price and volume movements.

### 2.1.2 Price impact based liquidity measures

Price impact refers to the change in the market price of a security that occurs as a result of executing an order. Price impact is a measure of liquidity, as it reflects the ease with which a trade can be executed without significantly affecting the market price. The larger the price impact, the less liquid the security is considered to be. Price impact is an important factor to consider for both market participants and researchers, as it affects the costs and returns associated with trading securities.

The Martin Index serves as a price impact measure, assessing the liquidity of a market by analyzing the link between trading volume and price movements. A high value for the Martin Index signifies poor liquidity, meaning that the price deviation in the observed time period is large compared to the traded volume. The Martin Index is mainly used to gauge the liquidity of a market as a whole, rather than for specific assets as stated by [35]. MI is given as:

$$MI = \sum_i^N \frac{(P_{i,n} - P_{i,n-1})^2}{V_{i,n}},$$

where  $P_{i,n}$  denotes the stock price and  $V_{i,n}$  is the transaction volume of the stock for a stock  $i$ , and for the day  $n$ .

Brunner (1996) [6] introduced a liquidity ratio that represents the average price change of a transaction over a given time period  $T$ . The formula for the ratio is:

$$LR = \frac{\sum_t^T |\Delta P_{i,t}|}{N_T}$$

where  $\Delta P_{i,t}$  represents the log return of the asset  $i$ , and  $N_T$  is the number of trades during the time period  $T$ . A lower value of this ratio indicates higher liquidity, as it

shows that the average price change per transaction is smaller. In cases where there are no trades occurring within the designated time period, the liquidity ratio becomes undefined. Assigning a value of zero to the ratio would inaccurately imply a high level of liquidity, which is not appropriate.

The illiquidity measure introduced by [2] is a widely used measure of price impact in finance literature [37]. The return to volume ratio is a metric that quantifies the relationship between the average daily price of a stock and its trading volume sensitivity. The ratio is calculated by averaging the daily impact of stock returns  $R_i$  on its volume  $V_i$  over a specified time period. To calculate the illiquidity ratio  $ILLR$  for stock  $i$ , the formula is as follows:

$$ILLR = \frac{1}{K} \sum_i^K \frac{|\Delta R_i|}{V_i}.$$

In comparison to other liquidity measures, the illiquidity ratio has some benefits. It is computed using daily return and volume data, which are easily obtainable, even in markets with limited transaction data. This enables long-term illiquidity ratio calculations by researchers, making it useful for analyzing most financial markets, including those in emerging economies. The ratio captures the relationship between trading volume and security price movements, converting it into transaction costs. An increase in trading volume is associated with a lower illiquidity ratio. The value of this ratio's ability to accurately assess price impact through its volume component is based on its correlation with trading volume [45].

Despite its usefulness as a measure of illiquidity, the return to volume ratio has some limitations. One such limitation is the size bias, where stocks with larger market capitalization are considered less illiquid simply because of their size. This makes it difficult to compare the illiquidity ratio among stocks with various market values [33]. Another limitation is that it fails to consider the impact of trading frequency on liquidity. This is becoming increasingly important, as trading frequency can significantly impact required liquidity premiums. However, the ratio  $ILLR$  assumes that trading frequency is similar across stocks, which is not always the case [23]. Thus, it may not provide a comprehensive picture of liquidity.

### 2.1.3 Transaction cost based liquidity measures

Transaction costs are the expenses incurred in the process of executing a trade. These costs can be divided into two types: explicit costs, which are identifiable and known before trading, such as order processing fees, taxes, and brokerage fees, and implicit costs, which are less noticeable but can make up a significant portion of the total transaction costs, including the bid-ask spread, the size of the transaction, and the timing of trade execution, which are less apparent but can make up a significant portion of the total transaction costs. Spread measures are commonly used to evaluate the cost of executing trades and the liquidity of a security or market. As the spread decreases, the implicit trading costs diminish, resulting in higher liquidity. Therefore, there is an inverse relationship between the spread size and the implicit trading costs. A smaller spread indicates higher liquidity in the market. There are three primary spread measures: quoted spread, effective spread and realized spread. The quoted spread refers to the difference between the quoted ask and bid prices that are provided in the market. The effective spread takes into account the actual price of trades and the quoted spread, while the realized spread reflects the actual difference between the buying and selling prices of a trade that was executed in the market.

The quoted spread is a measure of the cost of a complete transaction cycle in a financial market. It is calculated by subtracting the best bid price from the best ask price, and refers the implicit trading costs of buying and selling a security. A low quoted spread implies high liquidity in a market, as it means low implicit trading costs for small transactions. The quoted spread is particularly useful for orders that can be filled entirely at the best quotes, and it can be viewed as the trading costs for buyers or the trading profit for sellers. The quoted spread,  $QS$ , is:

$$QS = p_a - p_b$$

where  $p_a$  is for the best ask price and  $p_b$  is for the best bid price.

Although it is simple to compute, it is less representative of actual round-trip transaction costs for two reasons: (1) it assumes a short holding period for the asset, and (2) it does not consider any information from executed trades [54]. Despite these limitations, the quoted spread has the advantage of being able to be measured more

frequently due to the lack of required executed trade information, which can be particularly useful in markets where trade information is scarce, such as in the case of illiquid stocks.

The effective spread is a measure of the actual cost of a transaction, taking into account the actual transaction price. It is calculated by subtracting the midquote  $M_i$  at the time just prior to the transaction from the actual transaction price  $P_i$  for a stock  $i$ , and adjusting this difference by an order direction indicator that shows if the trade was started by the buyer ( $D_i = 1$ ) or the seller ( $D_i = -1$ ). The effective half-spread is then divided by the midquote to get the relative effective half-spread. This measure reflects the impact of a transaction on the market price. The effective spread,  $ES$ , is calculated as:

$$ES = D_i * (P_i - M_i).$$

The effective spread is calculated by taking into account actual prices and is often averaged over a specified time period, like a day or an hour, using a value-weighted method. This is done by determining the average of the effective spread, weighted by the dollar or euro volume of each trade observation.

The realized spread, ( $RS$ ), is a metric that quantifies the actual revenue earned by market makers. It is computed by subtracting the price impact of the initial trade over a fixed time horizon from the effective spread. Market makers are incentivized to quickly buy and sell assets in order to avoid holding inventory for extended periods of time, as adverse price movements could result in losses. This means that they may earn less than the effective spreads, as their profit margins are reduced by the need to quickly offload inventory. For the asset price  $P_n$  and mid-price  $M_n$  at time  $n$ , the realized spread,  $RS$ , is given as:

$$RS = 2 * |P_t - M_t|.$$

Roll (1984) [52] evaluates the appropriate spread by considering the first-order autocorrelation of price changes. This method is efficient and easy to use as it utilizes readily available market price time series. Roll's premise is that any price changes in an efficient market with no trading costs are the result of the disclosure of fresh information. Roll further assumes that in this market, regardless of prior trades, the

probability of a trade at the bid price is 50%. The exchange of transaction prices between bid and ask produces a negative first-order autocovariance of the price differences between consecutive transactions in this type of market, where only order processing contributes to the spread. Roll uses this relationship to derive a straight-forward spread estimator as given:

$$S = 2\sqrt{-cov(\Delta P_t, \Delta P_{t-1})}.$$

In order to account for the potential for serial covariance in the market's chain of trade initiations, [13] give a modified version of the Roll estimator. This describes the likelihood that a new trade will be initiated at the same price as the previous trade, whether at the bid price or the ask price. Based on their findings, they determined that the possibility of an extension occurring is greater than 50%, particularly when large market orders involve more than one counterparty, resulting in a single trade being recorded as multiple sequential trades. Therefore, the article proposed a modified Roll estimator to address this issue. The modified version is:

$$S = \frac{\sqrt{-cov(\Delta P_t, \Delta P_{t-1})}}{\pi}.$$

The value of  $\pi$  represents the probability of a trade reversal, meaning the possibility of a trade occurrence at a different price than the previous trade. A negative first-order auto covariance of transaction prices means that the changes in transaction prices over time are negatively correlated, which implies that large changes are followed by smaller changes and vice versa.

Beber and Pagano (2008) [5] highlight the advantage of using the bid-ask spread, which is that it provides information on the expected execution price of an order in a particular market, given the size of the order. However, they also acknowledge that this measure has a drawback in that it doesn't consider the impact that placing an order can have on market conditions, specifically the market price. According to [5], this is an important limitation of the bid-ask spread and other ex ante liquidity measures.

## **Implied liquidity**

In the wake of the recent credit crunch, assessing liquidity risk has become increasingly important for both market participants and regulators, as liquidity tends to dry up during periods of market turmoil. While the bid-ask spread of financial instruments is a widely used liquidity indicator, the non-linear relationship between volatility, spot price, and spread is widely acknowledged, as observed in various studies [20, 1]. This poses a limitation when measuring liquidity solely based on the underlying product's liquidity. To overcome this challenge, the law of two prices offers an alternative approach to gauge liquidity through the concept of implied liquidity. Corcuera et al. (2012) [20] propose this concept in the context of the Black-Scholes model. Implied liquidity gives investors the ability to quantify liquidity levels similarly to how implied volatility enables investors to assess market risk in terms of the standard deviation of the return distribution. This approach quantifies liquidity risk in a more fundamental way, allowing for comparisons across time, products, and asset classes. In this work, we use the implied liquidity as proxy for market liquidity level.





## CHAPTER 3

### PRELIMINARIES

In this chapter, we briefly give mathematical background related with the theory used in this work. In details, we review the Conic Finance Theory to explain the basics of the implied liquidity since we use the implied liquidity as a proxy for the market liquidity level. Then, we recall OU process and its exponential version.

#### 3.1 Conic Finance Theory

The two-price economy operates on a relatively classical view of markets, which aligns with its role in traditional competitive analysis. In this view, markets act as a counterparty to transactions. The primary difference from the traditional perspective is that the terms of trade are dependent on the direction of trade, with two different prices: ask is to buy from the market and bid is to sell to the market. The classical market enables trading in both directions at the prevailing market price and accepts all random cash flows at zero cost if they have a positive expectation under the equilibrium pricing kernel. This creates a large set of risks that the market accepts on a risk-neutral measure. However, the two-price market is more restrictive in its acceptance of trades. The market only accepts a smaller set of zero-cost risks, which are modeled as a convex cone containing the nonnegative random variables.

When modeling the two-price market, the market is regarded as a passive counterparty that accepts zero-cost trades suggested by opposite market participants. Cash flows for trades are viewed as bounded random variables on probability space  $(\Omega, \mathcal{F}, \mathbb{P})$ . A unique structure of cash flows acceptable to the market as a counterparty is formed

by the convex cone of cash flows accepted at zero cost.

The law of one price states that if a cash flow  $X$  is acceptable to the market with an expected value of zero, then trading occurs in both directions at the same price. This means that  $-X$  is also acceptable. The set of cash flows that are considered acceptable is determined by the half-space where the expected value of  $X$  is less than or equal to zero,  $E^{\mathbb{P}}(X) \geq 0$ . However, in two-price markets, we no longer assume that the law of one price holds. The set of cash flows that can be accepted at zero cost is denoted by the proper convex cone  $\mathcal{A}$ , which only contains non-negative cash flows. The size of this set is smaller than the set of the one-price economy. Furthermore, if  $X$  is acceptable, it may not be acceptable when the direction of trade is reversed ( $-X$ ) on the same terms.

The constructive description of the non-negative cash flows in the convex cones was established by [3]. They proved that a convex set  $\mathcal{M}$  of probability measures  $\mathbb{Q}$  belonging to  $\mathcal{M}$  and equivalent to  $\mathbb{P}$  exists, and any acceptable risks (cash flows) in set  $\mathcal{A}$  are denoted by  $X$  if and only if:

$$E^{\mathbb{Q}}[X] \geq 0 \quad \text{for any} \quad \mathbb{Q} \in \mathcal{M}.$$

The acceptability of cash flows is connected to a positive expectation through the use of concave distortion. To achieve this, a preferred concave distortion is selected, which is defined on the unit interval,  $0 \leq u \leq 1$ . Therefore, any concave distribution function  $\Psi(u)$  on the unit interval ( $u$ ) can be utilized to define a random variable  $X$  with a distribution function  $\mathcal{F}(x)$  and the distorted expectation of a risk  $X$  is

$$\int_{-\infty}^{\infty} x d\Psi(F_X(x)). \quad (3.1)$$

To construct models for markets, one approach is to define intersecting sets of supporting measures. However, this process is complex. In [12], the authors tackled this challenge by introducing operational cones that is dependent only on the distorted probability distribution of the cash flows. These cones enable the definition of a market as a convex cone of zero-cost acceptable cash flows, along with an associated convex set of probability measures  $\mathbb{Q} \in \mathcal{M}$ . In accordance with the proposal

by [12], the concept of distortion functions offers a practical approach to measuring acceptability. Distortion functions, denoted as  $\Psi$ , are mathematical functions that are both increasing and concave, mapping the unit interval  $[0, 1]$  onto itself. By applying a distortion function to a cumulative distribution function, it introduces a distortion effect based on a specific parameter value. The concavity of these distortion functions plays a crucial role in assigning weights to different outcomes of a random variable  $X$ . Lower outcomes are given higher weights, indicating their greater significance, while higher outcomes receive relatively lower weights. Consequently, as the parameter value increases, the distorted expectation of a cash flow  $X$  decreases, implying a diminishing impact on the overall value. In summary, utilizing a parametrized family of distortion functions allows for the practical measurement of acceptability by quantifying the distortion effect on the expectation of a cash flow. The concave nature of these functions ensures a more pronounced emphasis on lower outcomes, providing valuable insights into the impact and significance of different variables.

Equation (3.1) defines a cone of acceptable cash flows that is solely dependent on the distribution function of the cash flow and distortion function. The integral in (3.1) can be expressed as follows:

$$\int_{-\infty}^{\infty} x d\Psi'(F_X(x)) f(x) dx, \quad (3.2)$$

where  $f(x) = F'_X(x)$ .

When evaluating cash flows in the market, the concept of acceptability is linked to positive expectations using concave distortion. This can also be expressed as an expectation under a change of measure. It is worth noting that as  $\mathcal{F}(x)$  approaches zero, large losses are given higher weights by the function  $\Psi'(F_X(x))$ . As the distortion becomes more concave, the upward reweighing of losses increases, making it more difficult for cash flows to be deemed acceptable.

Cherny and Madan (2009) [12] introduced a family of concave distortion functions that vary with a real number  $\lambda$ . This  $\lambda$  value controls the level of concavity and the size of the set of acceptable cash flows. The cash flow  $X$  is considered acceptable if the stressed expectation remains positive under the given concave distortion. Equation (3.2) can be used to compute the concave distortion function numerically using

the distribution function of  $X$ . This computation can be simplified by using the empirical distribution function of a sample of observations  $x_1, x_2, \dots, x_N$ . This gives the following:

$$\int_{-\infty}^{\infty} x d\Psi(F_X(x)) = \sum_{n=1}^N x_n \left( \Psi^\lambda \left( \frac{n}{N} \right) - \Psi^\lambda \left( \frac{n-1}{N-1} \right) \right).$$

The index of acceptability or the measure of performance allows us to determine the cash flows that are acceptable at a certain level of  $\lambda$  (as described in [12]). This index is a non-negative real number that corresponds to a collection of terminal cash flows viewed as random variables that are acceptable at this level. According to [12], one way to construct the index of acceptability is by using a specific set of distortions. We will review the distortion functions given in [12].

### **Distortion functions:**

A concave distortion function refers to a concave function  $\Psi(u)$  that maps the unit interval to itself:  $\Psi : [0, 1] \rightarrow [0, 1] : u \mapsto \Psi(u)$ . The distortion functions are employed as a functional approach to compute the distorted expectations as given in (3.1). Thus, we briefly introduce some distortion functions given in [12].

i) The minvar distortion function: The minvar risk measure is linked to the acceptability index, which involves computing a sample as the expected value of the smallest selection from several choices in the cash flow distribution. The function is given:

$$\Psi_\lambda^{minvar}(u) = 1 - (1 - u)^{1+\lambda}, \quad \lambda \geq 0.$$

One of the downsides of minvar is that it assigns relatively small weight to large losses, making it not sufficiently relevant in economic theory. Consumers usually prefer to avoid risks, and large losses are particularly undesirable. However, this risk measure, minvar, is often regarded as too permissive towards risk and not sufficiently risk-averse to be considered a good risk measure. As a result, minvar is not commonly used as a risk measure in practice.

ii) The maxvar distortion function: The maxvar risk measure is linked to the acceptability index, which selects multiple items from the distribution and choosing the

highest one, this method results in the cash flow distribution. The function is given:

$$\Psi_{\lambda}^{maxvar}(u) = (1 - u) \frac{1}{1 + \lambda}, \quad \lambda \geq 0.$$

iii) The maxminvar distortion function: This approach can be perceived as creating a scenario where the worst outcome is anticipated, by initially adopting a maxvar perspective and subsequently employing a minvar perspective. The function is given:

$$\Psi_{\lambda}^{maxminvar}(u) = (1 - (1 - u)^{1+\lambda}) \frac{1}{1 + \lambda}, \quad \lambda \geq 0.$$

It does not take into account large gains and, as such, is not commonly used.

iv) The minmaxvar distortion function: This approach can be perceived as creating a scenario where the worst outcome is anticipated, by initially adopting a minvar perspective and subsequently employing a maxvar perspective.

$$\Psi_{\lambda}^{minmaxvar}(u) = 1 - (1 - u \frac{1}{1 + \lambda})^{1+\lambda}, \quad \lambda \geq 0.$$

The main advantage of this function is that it can preserve certain characteristics of the original distribution, such as the minimum, maximum and variance, which can be useful in certain situations where these features are important. However, it may result in a loss of information and details compared to the original distribution.

v) The Wang transform: It is a method used to transform a probability distribution in such a way that it can be used to generate scenarios that are more optimistic or more pessimistic than the original distribution. The Wang transform can be used in finance and economics to model financial risk and uncertainty, by shifting the distribution to the left or right, it allows for the generation of scenarios that are more likely or less likely to occur than the original distribution. More specifically, this process usually give more weight to the downside (losses) than to the upside (profits) compared to the original distribution function. The Wang transform is given as

$$\Psi_{\lambda}^{Wang}(u) = \Phi(\Phi^{-1}(u) + \lambda), \quad u \in [0, 1] \quad \lambda \geq 0.$$

### **Implied liquidity:**

Suppose the market accepts the risk  $X$  at the acceptability level  $L$  and its ask price is

$a_L$  and the bid price is  $b_L$ . They are given respectively [20]:

$$a_L(X) = - \int_{-\infty}^{\infty} x d\Psi^{(L)}(F_{-X}(x))$$

$$b_L(X) = \int_{-\infty}^{\infty} x d\Psi^{(L)}(F_X(x))$$

where Wang transform  $\Psi$  is given by

$$\Psi^L(y) = \Psi(\Psi^{-1}(y) + L), \quad y \in [0, 1] \quad L \geq 0.$$

The use of a concave distortion function ensures that the ask price is higher than the bid price. While there are several distortion functions available, the Wang transform is used as it assigns more weight to losses than profits, which is similar to the real market scenario.

Assume that  $S_t$  satisfies:

$$S_t = S_0 \exp\left(\left(\mu - \frac{\sigma^2}{2}\right)t + \sigma W_t\right) \quad t \geq 0,$$

then the bid price of a European call option  $C$  is given as ([39] Equations 15-16):

$$b_L(C) = S_t \exp(-L\sigma\sqrt{T-t})\Phi(d1) - \exp(-r(T-t))K\Phi(d2), \quad (3.3)$$

where  $d1 = \frac{\ln(S_t/K) - (r + \sigma^2/2)(T-t) + L\sigma\sqrt{T-t}}{\sigma\sqrt{T-t}}$  and  $d2 = d1 - \sigma\sqrt{T-t}$ .

The ask price is given as

$$a_L(C) = S_t \exp(L\sigma\sqrt{T-t})\Phi(d1) - \exp(-r(T-t))K\Phi(d2), \quad (3.4)$$

where  $d1 = \frac{\ln(S_0/K) + (r + \sigma^2/2)T - L\sigma\sqrt{T}}{\sigma\sqrt{T}}$  and  $d2 = d1 - \sigma\sqrt{T}$ .

For details and proofs, see [12, 20, 46].

The parameter  $L$ , matching the theoretical bid and ask prices with the real market prices, is called "implied liquidity" [47, 1].

### 3.2 The Ornstein-Uhlenbeck Process

Corcuera et al. (2012) [20], and Albrecher et al. (2013) [1] observed a mean-reverting behavior in the implied liquidity series. By following their suggestions, we consider to model implied liquidity as an exponential OU process that is the most basic

stochastic process explaining the characteristics of the process drift reverting to its long term value. The OU process is introduced by [59]. The model is also known as an arithmetic OU process.

Consider a probability space  $(\Omega, \mathcal{F}, \mathbb{F}, \mathbb{P})$  and an  $(\mathbb{F}, \mathbb{P})$  Brownian motion  $W_t$ .

**Definition 3.2.1.** (*Ornstein-Uhlenbeck process*). A stochastic process  $(X_t)_{t \geq 0}$  defined on the filtered probability space  $(\Omega, \mathcal{F}, \mathbb{F}, \mathbb{P})$  follows an (arithmetic) Ornstein-Uhlenbeck process with mean  $\mu$  satisfying the following Stochastic Differential Equation (SDE):

$$dX_t = \kappa(\mu - X_t)dt + \sigma dW_t \quad (3.5)$$

where  $\kappa$  denotes the mean reversion speed,  $\mu$  is the long run mean,  $\sigma$  denotes the volatility of the process and  $W_t$  is a standard Brownian motion.

The exact solution of (3.5) is obtained by applying Ito's Lemma.

**Theorem 3.2.1.** (*Ito's Lemma*) Given a diffusion process of the form

$$dX_t = \mu dt + \sigma dW_t$$

an a twice continuously differentiable function  $f(t, x)$  has the following dynamics:

$$df(t, X_t) = \left( \frac{\partial f}{\partial t} + \mu \frac{\partial f}{\partial x} + \frac{1}{2} \sigma^2 \frac{\partial^2 f}{\partial x^2} dW_t \right)$$

**Theorem 3.2.2.** The solution of the Ornstein-Uhlenbeck SDE in (3.5) is given by

$$X_t = X_0 e^{-\kappa t} + e^{-\kappa t} \mu (e^{\kappa t} - 1) + e^{\kappa t} \int_0^t \sigma e^{\kappa s} dW_s$$

*Proof.* By applying Ito's lemma to the function  $Y_t = e^{\theta t} X_t$ , we obtain

$$dY_t = \kappa e^{\kappa t} X_t dt + e^{\kappa t} dX_t = \kappa e^{\kappa t} X_t dt + e^{\kappa t} (\kappa(\mu - X_t) dt + \sigma dW_t)$$

gives that

$$= \kappa e^{\kappa t} \mu dt + e^{\kappa t} \sigma dW_t$$

Rewriting the formula in integral form gives

$$Y_t = Y_0 + \int_0^t \sigma e^{\kappa s} \mu ds + \int_0^t \sigma e^{\kappa s} dW_s = Y_0 + \mu(e^{\kappa t} - 1) + \int_0^t \sigma e^{\kappa s} dW_s$$

$$Y_t = e^{\kappa t} X_t \Rightarrow X_t = e^{-\kappa t} Y_t$$

$$X_t = e^{-\kappa t} Y_t = X_0 e^{-\kappa t} + e^{-\kappa t} \mu (e^{\kappa t} - 1) + e^{-\kappa t} \int_0^t \sigma e^{\kappa s} dW_s$$

By rearranging the terms of the above equation we get the solution to the OU SDE:

$$X_t = X_0 e^{-\kappa t} + e^{-\kappa t} \mu (e^{\kappa t} - 1) + e^{-\kappa t} \int_0^t \sigma e^{\kappa s} dW_s$$

□

$X_t$  is normally distributed with

$$\mathbb{E}(X_t) = \mu + (X_0 - \mu)e^{-\kappa t} \quad \text{and} \quad \text{var}(X_t) = \frac{\sigma^2}{2\kappa}(1 - e^{-2\kappa t}).$$

For  $0 \leq s \leq t$ , the covariance is

$$\text{Cov}(X_t, X_s) = \frac{\sigma^2}{2\kappa}(e^{-\kappa|t-s|} - e^{-\kappa(t+s)}).$$

Table 3.1: Parameters used in simulation

$g$	$\varsigma$	$\kappa$	$T$	$\Delta$	$N$
2	0.5	5	10	1/250	$T/\Delta$

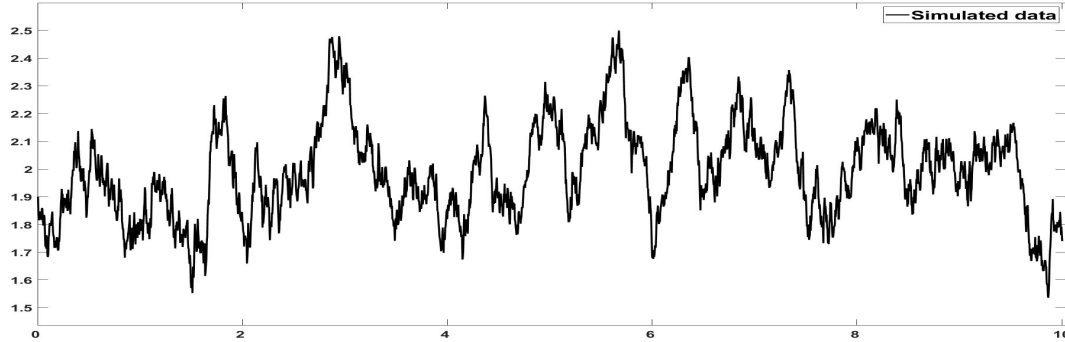


Figure 3.1: Simulated path - OU process

We provide a simulated path of an arithmetic OU process with the parameter set in the Table 3.1 in the Figure 3.1.

### 3.2.1 Exponential Ornstein-Uhlenbeck Process

The arithmetic OU process is not a suitable model for asset prices, as it can take negative values with positive probability. This problem is overcome by [55] with a modification of arithmetic model: exponential (geometric) OU process (also known as equilibrium one factor model, or Schwartz reduced form).



**Definition 3.2.2.** (*Exponential Ornstein-Uhlenbeck process*) A stochastic process  $X_t$  defined on the filtered probability space  $(\Omega, \mathcal{F}, \mathbb{F}, \mathbb{P})$  is an exponential OU process if it satisfies the following stochastic differential equation:

$$dX_t = \kappa(\mu - \ln(X_t))X_t dt + \sigma X_t dW_t. \quad (3.6)$$

**Lemma 3.2.1.** Suppose  $X$  follows an exponential OU process, then the process  $Y = \ln(X)$  follows an OU process.

*Proof.*

$$dX_t = \kappa(\alpha - \ln(X_t))X_t dt + \sigma X_t dW_t. \quad (3.7)$$

Apply Ito's lemma to  $f(X_t) = \ln(X_t)$

$$\begin{aligned} d\ln(X_t) &= \frac{\partial f(X_t)}{\partial t} dt + \frac{\partial f(X_t)}{\partial X_t} dX_t + \frac{1}{2} \frac{\partial^2 f(X_t)}{\partial X_t^2} dX_t^2 \\ &= \frac{\partial \ln X_t}{\partial t} dt + \frac{\partial \ln X_t}{\partial X_t} dX_t + \frac{1}{2} \frac{\partial^2 \ln X_t}{\partial X_t^2} dX_t^2 \\ &= 0 dt + \frac{1}{X_t} dX_t - \frac{1}{2X_t^2} (dX_t)^2 \\ &= \kappa(\mu - \ln X_t) dt + \sigma dW_t - \frac{1}{2} \sigma^2 dt \\ &= \kappa(\mu - \frac{1}{2\kappa} \sigma^2 - \ln X_t) dt + \sigma dW_t \\ &= \kappa(\alpha - \ln X_t) dt + \sigma dW_t, \quad \text{where} \quad \alpha = \mu - \frac{1}{2\kappa} \sigma^2 \end{aligned}$$

Let  $Y_t = \ln(X_t)$

$$dY_t = \kappa(\alpha - Y_t) dt + \sigma dW_t. \quad (3.8)$$

□

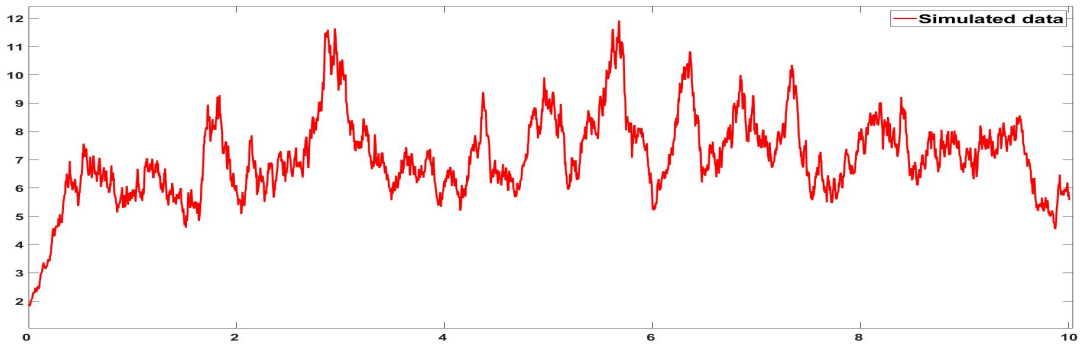


Figure 3.2: Simulated path - Exponential OU process

A simulated path of an exponential OU process with the parameter set in the Table 3.1 is given in Figure 3.2.

## CHAPTER 4

### MODEL AND ESTIMATION

In this chapter, we introduce our approach to estimate the unknown parameters in the Markov chain modulated OU model. First, we provide the notation and setting required to introduce our model. To make a statistical inference for a hidden Markov model, we use the Expectation Maximization (EM) algorithm. Accordingly, we review the EM algorithm for Markov chain modulated OU process given in [28]. Note that the proofs are not provided in [28]. For the thesis to be self contained, we provide them in detail. The implementation of the algorithm needs the filters that depend on the observations continuously. These filters are known as robust filters [17, 42]. Thus, we derive the robust filters for our framework by following the idea introduced in [17, 42]. This approach provides a discrete time setting however it has an explicit approximation of the continuous time filters. Finally, working with discretized robust filters makes it possible to introduce the variance estimate of the model, which is not possible to estimate in the continuous time model setting.

#### 4.1 Model setting and notation

This part gives the notation and dynamics of OU process which is modulated by a continuous-time hidden Markov chain. Then, we give basic idea of the EM algorithm.

**The state process:** We assume a continuous-time finite-state Markov chain  $X = \{X_t; 0 \leq t \leq T\}$  defined on a filtered probability space  $(\Omega, \mathcal{F}, \mathbb{F}, \mathbb{P})$  where  $\mathbb{F} = (\mathcal{F}_t)_{(0 \leq t \leq T)}$  is the global filtration that satisfies the usual conditions. All processes are  $\mathbb{F}$ -adapted.  $X$  has a state space  $S = \{e_1, e_2, \dots, e_K\}$  where  $e_k$  is the  $k^{\text{th}}$  basis

column vector of  $\mathbb{R}^K$ . The transpose of its infinitesimal generator (transition rate matrix) is denoted by  $A$ . Thus, we have  $A = (a^{ij})$  such that, for  $i \neq j$ ,  $a^{ij} \geq 0$ ,  $a^{jj} = -\sum_{i \neq j}^K a^{ij}$ ,  $i, j \in \{1, \dots, K\}$  and, its probability distribution is  $\pi_t = (\pi_t^1, \dots, \pi_t^K)$  which satisfies the forward equation  $\frac{d\pi_t}{dt} = A_t \pi_t$  with given initial probability  $\pi_0$ . Then, the state process  $X$  can be written as the following semimartingale form

$$X_t = X_0 + \int_0^t A X_s ds + M_t \quad (4.1)$$

where  $M_t$  is a  $\mathbb{F}$ -martingale under  $\mathbb{P}$ .

**The observation process:** Corcuera et al. (2012) [20] observed that implied liquidity illustrates a mean reverting behavior, which is also supported by [1]. Then, following the idea by [1] and [20], we assume that implied liquidity  $L$  follows a Markov-chain modulated exponential OU process:

$$dL_t = \kappa \left( \tilde{g}(X_t) + \frac{\varsigma^2}{2} - \log(L_t) \right) L_t dt + \varsigma L_t dW_t, \quad (4.2)$$

where  $\kappa > 0$  is the mean reversion speed,  $\tilde{g}(X_t)$  is the long-run mean reversion level, and  $\varsigma$  is the volatility of the noise.  $W$  is a standard  $\mathbb{P}$ -Brownian motion with respect to  $\mathbb{F}$  which is independent of  $X$ . We assume that the Markov chain  $X$  representing the true market liquidity level is not directly observable, and the market participants observe only the (log) implied liquidity given in (4.2). Here we point out that the regime changes on true market liquidity have an impact on the long-run equilibrium level of implied liquidity, thus we modulate the mean level  $\tilde{g}$  with the Markov chain  $X$ , i.e.  $\tilde{g}(X)$ .

When we apply Ito's formula to  $\log(L_t) = Y_t$  in (4.2), we get

$$dY_t = \kappa(\tilde{g}(X_t) - Y_t)dt + \varsigma W_t. \quad (4.3)$$

Note that variant of this model (without Markov-chain modulation) is also known as Schwartz reduced-form [55].

The information accessible to the observer of the system is conveyed through the sigma algebra generated by the filtration  $\mathbb{Y}$ , that is

$$\mathbb{Y} = (\mathcal{Y}_t)_{t \geq 0}, \quad \mathcal{Y}_t = \sigma\{L_s, 0 \leq s \leq t\} = \sigma\{Y_s, 0 \leq s \leq t\}.$$

The full information of the system is generated by the global filtration, i.e.

$$\mathbb{F} = (\mathcal{F}_t)_{t \geq 0}, \quad \mathcal{F}_t = \sigma\{L_s, X_s, 0 \leq s \leq t\} = \sigma\{Y_s, X_s, 0 \leq s \leq t\}.$$

Then, we define the *normalized observation* process  $y_t = Y_t/\varsigma$  and denote by  $g = \tilde{g}(\cdot)/\varsigma$ , we get:

$$dy_t = \kappa(g(X_t) - y_t)dt + W_t. \quad (4.4)$$

Note that  $\mathcal{Y}_t \subset \mathcal{F}_t$ ,  $t \geq 0$ . For an integrable and measurable process  $H$ ,  $\hat{H}_t := E[H_t | \mathcal{Y}_t]$  *a.s.*, the  $\mathbb{Y}$ -optional projection, gives the filtered estimate of  $H_t$ . For a generic function  $f$  it holds that  $f(X_t) = \langle X_t, \mathbf{f} \rangle$  where  $\langle \cdot, \cdot \rangle$  denotes the scalar product and  $\mathbf{f}_k = f(e_k)$ ,  $1 \leq k \leq K$ , so that functions of the Markov chain can be identified with  $K$ -vectors.

**EM algorithm:** Here, we review the EM algorithm. The EM algorithm is a useful tool for finding the maximum likelihood estimates (MLEs) of parameters in statistical models. These models often involve unknown parameters, known data observations, and latent variables. The EM algorithm proceeds in iterations, with each iteration consisting of two steps. The first step is the expectation step (E-step), where the algorithm creates a function that estimates the conditional expectation of the log-likelihood (filtered log-likelihood) function based on the available information using the current parameters. In the second step, called the maximization step (M-step), the algorithm finds the parameters that maximize the log-likelihood function computed in the E-step. In the following E-step, the distribution of the latent (hidden) variables is calculated using the new parameter estimates. The EM algorithm can converge to a local maximum of the likelihood function and it provides estimates for the unknown parameters. The algorithm iterates between two steps until a given convergence criterion is met for the sequence of MLEs.

Let  $\theta$  denote the set of unknown parameters and  $\Theta$  denote the set of admissible parameters such that  $\theta \in \Theta$ .  $\mathbb{P}_\theta$  is the corresponding probability measure which is absolutely continuous with respect to the fixed probability measure  $\mathbb{P}_{\theta_0}$ , where  $\theta_0$  is the initial parameter set. The algorithm starts with the initial parameter set  $\theta_0$  to obtain an estimate of the parameter set  $\theta_1$ . The iterative estimation procedure produces

a sequence of parameter estimates  $\{\theta_n\}_{n \in N}$ . The main steps of the algorithm are summarized as follows:

**E-step:** Set  $\theta^* = \theta_n$  and compute the filtered loglikelihood function

$$\widehat{L}(\theta, \theta^*) = E_{\theta^*}(\log \frac{d\mathbb{P}_\theta}{d\mathbb{P}_{\theta^*}} | \mathcal{Y}_T) \quad \text{for all } \theta, \theta^* \in \Theta.$$

**M-step:** Maximize  $\widehat{L}(\theta, \theta^*)$  to find  $\theta_{n+1}$ , i.e.

$$\theta_{n+1} \in \operatorname{argmax}_{\theta \in \Theta} \widehat{L}(\theta, \theta^*).$$

#### 4.1.1 EM algorithm for the current setting

The estimation problem aims to have the MLEs for the unknown parameters  $A$ ,  $g$  and  $\kappa$ . The EM methodology for OU process follows from [28]. First, we introduce several processes that are required in the E-step of the algorithm.

i)  $J_t^i$  is the occupation time of the state of the Markov chain in state  $i$  until time  $t$ :

$$J_t^i = \int_0^t \langle X_r, e_i \rangle dr. \quad (4.5)$$

ii)  $N_t^{ij}$  is the number of transitions from state  $i$  to  $j$  of the process  $X$  where  $i \neq j$  up to time  $t$ :

$$N_t^{ij} = \int_0^t \langle X_r, e_i \rangle \langle dX_r, e_j \rangle. \quad (4.6)$$

iii)  $G_t^i$  is the level sum of the integral for state  $e_i$  until time  $t$ :

$$G_t^i = \int_0^t \langle X_r, e_i \rangle dy_r. \quad (4.7)$$

iv)  $I_t^i$  is the auxiliary process for the state  $i$  until the time  $t$ :

$$I_t^i = \int_0^t y_r \langle X_r, e_i \rangle dr. \quad (4.8)$$

**a) E-step:**

Suppose that the estimation step starts with a parameter set

$$\theta^* = (a^{*ij}, g^{*i}, \kappa^*, 1 \leq i, j \leq N).$$

Then, we estimate the new parameter set

$$\theta = (a^{ij}, g^i, \kappa, 1 \leq i, j \leq N),$$

which maximizes the log-likelihood function. Denote by  $\mathbb{P}_{\theta^*}$  and  $\mathbb{P}_\theta$  the corresponding probability measures implied by  $\theta^*$  and  $\theta$ .

We have that

$$\begin{aligned} \widehat{L}(\theta, \theta^*) = E\left[\log \frac{dP_\theta}{dP_{\theta^*}} \mid \mathcal{Y}_T\right] &= \sum_{i=1}^N (\kappa g^i \hat{G}_T^i - \frac{1}{2} \kappa g^{i^2} \hat{J}_T^i + \kappa g^i \hat{I}_T^i) \\ &+ \sum_{\substack{i \neq j \\ i, j=1}}^N (\hat{N}_T^{ij} \log(a^{ji}) - a^{ji} \hat{J}_T^i) + \hat{R}(\theta^*), \end{aligned} \quad (4.9)$$

where  $\hat{R}(\theta^*)$  is independent of  $\theta$ .

### b) Maximization step:

In the maximization step of the algorithm, the updates from  $A^*, g^*, \kappa^*$  to  $A, g, \kappa$  are given by

i) The estimate of  $a^{ji}$ :

$$\hat{a}^{ji} = \frac{\hat{N}_T^{ij}}{\hat{J}_T^i}. \quad (4.10)$$

ii) The estimate for  $\kappa$ :

$$\hat{\kappa} = \frac{C}{D} \quad (4.11)$$

where

$$\begin{aligned} C &= \int_0^T y_s dy_s - \sum_{i=1}^N \frac{\hat{I}_T^i \hat{G}_T^i}{\hat{J}_T^i} \\ D &= \sum_{i=1}^N \frac{(\hat{I}_T^i)^2}{\hat{J}_T^i} - \int_0^T y_s^2 dy_s. \end{aligned}$$

iii) The estimate for  $g^i$ :

$$\hat{g}^i = \frac{\hat{\kappa}^{-1} \hat{G}_T^i + \hat{I}_T^i}{\hat{J}_T^i}. \quad (4.12)$$

In the following, we show how to obtain MLEs given in (4.10) to (4.12).

### The derivation of the MLEs of unknown parameters

The computation of the EM algorithm is based on the filtered estimates in (4.9). We need to find the expression for  $\frac{d\mathbb{P}_\theta}{d\mathbb{P}_{\theta^*}}$  where

$$\theta^* = (a^{*ij}, g^{*i}, \kappa^*, 1 \leq i, j \leq K).$$

and

$$\theta = (a^{ij}, g^i, \kappa, 1 \leq i, j \leq K).$$

are two possible parameter sets. Now,

$$\begin{aligned} \left. \frac{d\mathbb{P}_\theta}{d\mathbb{P}_{\theta^*}} \right|_{\mathcal{F}_t} &= \exp \left[ \int_0^t (\kappa \langle X_r, g \rangle - y_r) - \kappa^* (\langle X_r, g^* \rangle - y_r) dy_r \right. \\ &\quad \left. - \frac{1}{2} \int_0^t (\kappa^2 \langle X_r, g \rangle^2 - \kappa^{*2} \langle X_r, g^* \rangle^2) dr \right] \\ &\quad \times \prod_{i,j=1}^K \left( \frac{a^{ji}}{a^{ji^*}} \right)^{N^{ij}} \exp \left( \int_0^t (a^{ji} - a^{ji^*}) \langle X_r, e_i \rangle dr \right). \end{aligned}$$

Given the observations  $y_t$ ,  $0 \leq t \leq T$ , the partial information loglikelihood function becomes

$$\begin{aligned} L(\theta, \theta^*) &= E \left[ \log \frac{dP_\theta}{dP_{\theta^*}} | \mathcal{Y}_T \right] \tag{4.13} \\ &= \kappa \left[ \left( E \int_0^T \langle X_r, g \rangle dy_r | \mathcal{Y}_T \right) - \left( E \int_0^T y_r dy_r | \mathcal{Y}_T \right) \right] \\ &\quad - \frac{1}{2} \kappa^2 \left[ E \left( \int_0^T \langle X_r, g \rangle^2 dr | \mathcal{Y}_T \right) - 2E \left( \int_0^T y_r \langle X_r, g \rangle dr | \mathcal{Y}_T \right) \right. \\ &\quad \left. + E \left( \int_0^T y_r^2 dr | \mathcal{Y}_T \right) \right] \\ &\quad + \sum_{\substack{i \neq j \\ i,j=1}}^K \left( \log(a^{ji}) E(N_T^{ij} | \mathcal{Y}_T) - a^{ji} E \left( \int_0^T \langle X_r, e_i \rangle dr | \mathcal{Y}_T \right) \right) + \hat{R}(\theta^*), \end{aligned}$$

where  $\hat{R}(\theta^*)$  is the remainder term independent of  $\theta$ .

Note that  $\langle X_r, g \rangle = \sum_{i=1}^K g^i \langle X_r, e_i \rangle$  and  $\langle X_r, g \rangle^2 = \sum_{i=1}^K g^{i2} \langle X_r, e_i \rangle$ . The simplified



form of (4.13) can be written as

$$\begin{aligned}
L(\theta, \theta^*) &= \sum_{i=1}^K \kappa g^i E \left( \int_0^T \langle X_r, e_i \rangle dy_r | \mathcal{Y}_T \right) \\
&\quad - \sum_{i=1}^K \frac{1}{2} \kappa^2 g^{i^2} E \left( \int_0^T \langle X_r, e_i \rangle dy_r | \mathcal{Y}_T \right) \\
&\quad + \sum_{i=1}^K \kappa^2 g^i E \left( \int_0^T y_r \langle X_r, e_i \rangle dr | \mathcal{Y}_T \right) \\
&\quad + \sum_{\substack{i \neq j \\ i, j=1}}^K \left( \log(a^{ji}) E(N_T^{ij} | \mathcal{Y}_T) - a^{ji} E \left( \int_0^T \langle X_r, e_i \rangle dr | \mathcal{Y}_T \right) \right) + \hat{R}(\theta^*).
\end{aligned} \tag{4.14}$$

We can rewrite (4.14) by replacing the conditional expectations of the quantities in (4.5) to (4.8).

Then, the Equation (4.14) becomes

$$\begin{aligned}
\widehat{L}(\theta, \theta^*) &= E \left[ \log \frac{dP_\theta}{dP_{\theta^*}} | \mathcal{Y}_T \right] = \sum_{i=1}^N (\kappa g^i \hat{G}_T^i - \frac{1}{2} \kappa g^{i^2} \hat{J}_T^i + \kappa g^i \hat{I}_T^i) \\
&\quad + \sum_{\substack{i \neq j \\ i, j=1}}^N (\hat{N}_T^{ij} \log(a^{ji}) - a^{ji} \hat{J}_T^i) + \hat{R}(\theta^*).
\end{aligned} \tag{4.15}$$

Then, we maximize  $L(\theta, \theta^*)$  with respect to  $\theta$ . This means that we equate the partial derivatives of (4.15) with respect to  $g^i$ ,  $a^{ji}$  and  $\kappa$  to zero. After necessary simplifications, we obtain the estimates for the model parameters as

$$\begin{aligned}
\hat{a}^{ji} &= \frac{\hat{N}_T^{ij}}{\hat{J}_T^i} \\
\hat{\kappa} &= \frac{C}{D}
\end{aligned}$$

where

$$\begin{aligned}
C &= \int_0^T y_s dy_s - \sum_{i=1}^N \frac{\hat{I}_T^i \hat{G}_T^i}{\hat{J}_T^i} \\
D &= \sum_{i=1}^N \frac{(\hat{I}_T^i)^2}{\hat{J}_T^i} - \int_0^T y_s^2 dy_s \\
\hat{g}^i &= \frac{\hat{\kappa}^{-1} \hat{G}_T^i + \hat{I}_T^i}{\hat{J}_T^i}.
\end{aligned}$$

## 4.2 Filtering

In order to execute the EM algorithm, it is necessary to acquire filtered estimates of the quantities in Equation 4.15. This is a non-linear filtering problem. To address this problem, we first review the continuous time filters for the OU process and then we introduce the robust filters of the processes (4.5) - (4.8).

### 4.2.1 Continuous time filters

In this part, we review the continuous time filters derived in [28]. They present non-linear filtering results that are required in the EM algorithm to obtain the unknown parameters in the OU model. In [28], first the normalized filters are obtained by the innovation approach, then the corresponding unnormalized filters are introduced. Note that the proofs are not provided in [28]. For the thesis to be self contained, we provide them below in detail. First, we will recall the main results with their proofs on the general finite-dimensional filters given in [28].

**Theorem 4.2.1.** (Theorem 1 in [29]) Consider the process  $H = \{H_t; 0 \leq t \leq T\}$  described as

$$H_t = H_0 + \int_0^t \alpha_r dr + \int_0^t \delta_r dW_r + \int_0^t \beta_r dM_r \quad (4.16)$$

where  $\alpha$  and  $\delta$  are  $\mathbb{F}$ -predictable scalar processes and  $\beta$  is  $\mathbb{F}$ -predictable  $K$  dimensional vector process. Furthermore,

$$E \left[ \int_0^T (|\alpha_r| + |\delta_r|)^2 dr \right] + E \left[ \int_0^T \sum_{i=1}^K |\beta_r^i| dr \right] < \infty.$$

Then  $\hat{H}$  has a form

$$\hat{H}_t = \hat{H}_0 + \int_0^t \hat{\alpha}_r dr + \int_0^t \mu_r^1 dw_r \quad (4.17)$$

where

$$\mu_r^1 = \hat{\delta}_r + \kappa(\langle X_r, g \rangle - \widehat{y_r})\hat{H}_r - \kappa(\langle \hat{X}_r, g \rangle - y_r)\hat{H}_r. \quad (4.18)$$

*Proof.* The following properties are used for the proof.

1. For every  $\mathbb{F}$ -martingale  $M$ , the projection  $\hat{M}$  is  $\mathbb{Y}$ -martingale.

2. For a  $\mathbb{F}$ -adapted, integrable process  $\alpha$ , the process

$$\left( \widehat{\int_0^t \alpha_r dr} - \int_0^t \hat{\alpha}_r dr \right)_{0 < t < T}$$

is a  $\mathbb{Y}$ -martingale.

3. For every  $\mathbb{F}$ -martingale  $\mu$ , there is a  $\mathbb{F}$ -predictable process  $\gamma$  such that

$$\gamma_t = \gamma_0 + \int_0^t \mu_r dw_r.$$

Property (1) and Property (2) are standard in the nonlinear-filtering literature, the proof of Property (3) can be found in [19]. Using Property (1) and Property (2), we write

$$\hat{H}_t = \hat{H}_0 + \int_0^t \hat{\alpha}_r dr + \gamma_t$$

for some  $\mathbb{Y}$ -martingale  $\mu$ . Using Property (3) gives that

$$\hat{H}_t = \hat{H}_0 + \int_0^t \hat{\alpha}_r dr + \int_0^t \mu_r^1 dw_r. \quad (4.19)$$

Now, we need to identify the integrand  $\mu^1$ . The observation process  $y$  can be written either as

$$dy_t = \kappa(\langle X_t, g \rangle - y_t) dt + W_t. \quad (4.20)$$

or in innovations form

$$dy_t = \kappa(\langle \hat{X}_r, g \rangle - y_t) dt + w_t. \quad (4.21)$$

where the innovations process is represented by the Brownian motion process  $w$  [29].

From [4.16] and [4.20], applying Ito's product rule, we have

$$y_t H_t = \int_0^t y_r \alpha_r dr + \int_0^t \kappa(\langle X_r, g \rangle - y_r) H_r dr + \int_0^t \delta_r dr + \gamma_t^1 \quad (4.22)$$

where  $\gamma^1$  is an  $\mathbb{F}$ -martingale. Then using (1) and (2), we have the dynamics for  $\widehat{y_t H_t}$

$$\widehat{y_t H_t} = \int_0^t y_r \hat{\alpha}_r dr + \int_0^t \kappa(\langle X_r, g \rangle - \widehat{y_r}) \widehat{H_r} dr + \int_0^t \hat{\delta}_r^1 dr + \gamma_t^2 \quad (4.23)$$

where  $\gamma^2$  is an  $\mathbb{F}$ -martingale.

Moreover, it holds that  $\widehat{y_t H_t} = y_t \widehat{H_t}$  as  $y$  is  $\mathbb{Y}$ -adapted. From (4.19) and (4.21), applying Ito's product rule, we get

$$y_t \widehat{H_t} = \int_0^t y_r \widehat{\alpha_r} dr + \int_0^t \kappa(\langle \widehat{X_r}, g \rangle - y_r) \widehat{H_r} dr + \int_0^t \mu_r^1 dr + \gamma_t^3 \quad (4.24)$$

where  $\gamma^3$  is an  $\mathbb{F}$ -martingale.

As  $\widehat{y_t H_t}$  is a special semimartingale and has a unique decomposition (see [51], Chapter 7, Theorem 34),  $\widehat{y_t H_t} = y_t \widehat{H_t}$ , the finite variation and martingale parts in (4.23) and (4.24) must be equal. Thus, equating the integrands, we get

$$\mu_r^1 = \widehat{\delta_r} + \kappa(\langle X_r, g \rangle - y_r) H_r - \kappa(\langle \widehat{X_r}, g \rangle - y_r) \widehat{H_r}.$$

□

Note that the integrand  $\mu_r^1$  includes the  $\langle X_r, g \rangle H_r$  which is not recursive. [29] considers a filter for  $(H_t X_t)_{t \geq 0}$  to overcome this problem. In the following, we follow this idea and provide the filter for the process  $(H_t X_t)_{t \geq 0}$  for the case with the observation process given in (4.4).

**Proposition 4.2.1.1.**

$$\begin{aligned} \widehat{H_t X_t} &= \widehat{H_0 X_0} + \int_0^t \widehat{\alpha_r X_r} dr + \int_0^t \widehat{H_r A X_r} dr \\ &\quad + \sum_{i,j=1}^K \int_0^t \langle \widehat{\beta_r^j X_r} - \widehat{\beta_r^i X_r}, e_i \rangle a_{ji} dr (e_j - e_i) \\ &\quad + \int_0^t \mu_r^2 dw_r \end{aligned}$$

where

$$\mu_r^2 = \widehat{\delta_r X_r} + \kappa(\langle X_r, g \rangle - y_r) H_r X_r - \kappa(\langle \widehat{X_r}, g \rangle - y_r) \widehat{H_r X_r}.$$

*Proof.* Using (4.16) and (4.1) and applying Ito's product rule, we obtain

$$\begin{aligned} H_t X_t &= H_0 X_0 + \int_0^t \alpha_r X_r dr + \int_0^t \beta_r X_{r-} dM_r + \int_0^t \delta_r X_{r-} dW_r \\ &\quad + \int_0^t H_r A X_r dr + \int_0^t H_{r-} dM_r + \sum_{0 < r \leq t} (\beta_r \Delta X_r) \Delta X_r. \end{aligned}$$

Note that  $[H, X]_t = \sum_{0 < r \leq t} (\beta_r \Delta X_r) \Delta X_r$  and

$$\sum_{0 < r \leq t} (\beta_r \Delta X_r) \Delta X_r = \sum_{i,j=1}^K \int_0^t \langle \widehat{\beta_r^j X_r} - \widehat{\beta_r^i X_r}, e_i \rangle a_{ji} dr (e_j - e_i) + M_t$$

for some  $\mathbb{F}$ -martingale  $M$ , for the proof see ([29], Theorem 2).

Theorem 4.2.1 can be applied to  $H = HX$  with

$$\begin{aligned} \alpha_r &= \alpha_r X_r + H_r A X_r + \sum_{i,j=1}^K \int_0^t \langle \widehat{\beta_r^j X_r} - \widehat{\beta_r^i X_r}, e_i \rangle a_{ji} dr (e_j - e_i) \\ \delta_r &= \delta_r X_{r-}. \end{aligned}$$

$\beta$  does not appear in  $\mu_r^1$ . From Theorem 4.2.1,

$$\begin{aligned} \widehat{H_t X_t} &= \widehat{H_0 X_0} + \int_0^t \widehat{\alpha_r X_r} dr + \int_0^t \widehat{H_r A X_r} dr \\ &\quad + \sum_{i,j=1}^K \int_0^t \langle \widehat{\beta_r^j X_r} - \widehat{\beta_r^i X_r}, e_i \rangle a_{ji} dr (e_j - e_i) \\ &\quad + \int_0^t \mu_r^2 dw_r \end{aligned}$$

where

$$\mu_r^2 = \widehat{\delta_r X_r} + \kappa(\langle X_r, g \rangle - y_r) H_r X_r - \kappa(\langle \hat{X}_r, g \rangle - y_r) \widehat{H_r X_r}.$$

Moreover,

$$\langle X_r, g \rangle X_r = \sum_{k=1}^K \langle X_r, e_k \rangle g_k e_k$$

Similarly,

$$(\langle \widehat{X_r}, g \rangle) H_r X_r - y_r \widehat{H_r X_r} = \sum_{k=1}^K \langle H_r X_r, e_k \rangle g_k e_k - y_r \widehat{H_r X_r} = B_r \widehat{H_r X_r}.$$

$$\begin{aligned} \widehat{H_t X_t} &= \widehat{H_0 X_0} + \int_0^t \widehat{\alpha_r X_r} dr + \int_0^t \widehat{H_r A X_r} dr \\ &\quad + \sum_{i,j=1}^K \int_0^t \langle \widehat{\beta_r^j X_r} - \widehat{\beta_r^i X_r}, e_i \rangle a_{ji} dr (e_j - e_i) \\ &\quad + \int_0^t (\widehat{\delta_r X_r} + \kappa B_r \widehat{H_r X_r} - \kappa(\langle \hat{X}_r, g \rangle - y_r) \widehat{H_r X_r}) dw_r \end{aligned} \tag{4.25}$$

□

The filter in (4.25) is also called as normalized filter of  $(H_t X_t)_{t \geq 0}$ . In order to obtain robust filters introduced later in Section (4.2.2), one needs the dynamics of unnormalized filters. The unnormalized filters are linear and directly driven by the observation process  $y$ . To derive unnormalized filters, we first introduce a new probability measure.

Assume that there is a probability measure  $\bar{\mathbb{P}}$  on  $(\Omega, \mathcal{F}_T)$  under which  $X$  is a finite state Markov chain with the transpose of the intensity matrix  $A$  and  $w = \{w_t = y_t; 0 \leq t \leq T\}$  is a Brownian motion independent of  $X$ . Consider the reference probability measure  $\bar{\mathbb{P}}$  such that  $\mathbb{P} \sim \bar{\mathbb{P}}$  and the corresponding Radon-Nikodym derivative of  $\mathbb{P}$  with respect to probability measure  $\bar{\mathbb{P}}$  is given by

$$\left. \frac{d\mathbb{P}}{d\bar{\mathbb{P}}} \right|_{\mathcal{F}_t} = \Lambda_t.$$

where

$$\Lambda_t = \exp \left\{ \int_0^t \kappa \langle X_s, g \rangle dy_s - \frac{1}{2} \int_0^t \kappa^2 \langle X_s, g \rangle^2 ds \right\}. \quad (4.26)$$

According to Girsanov's theorem, the process  $dW_t = dy_t - \kappa(\langle X_t, g \rangle - y_t)dt$ ,  $W_0 = 0$  is a  $\mathbb{P}$ -Wiener process and independent of  $X$ . That is, the process  $y$  is a standard Brownian motion under the probability measure  $\bar{\mathbb{P}}$ , while the dynamics of Markov chain does not change under  $\bar{\mathbb{P}}$ . Working under the reference probability measure  $\bar{\mathbb{P}}$  makes the calculations easier since the observation process  $y$  becomes a Wiener process. To summarize, under the measure  $\mathbb{P}$ , the dynamics of the Markov chain  $X$  and the observation process  $y$  are:

$$\begin{aligned} dX_t &= AX_t dt + dM_t \\ dy_t &= \kappa(\langle X_t, g \rangle - y_t)dt + dW_t. \end{aligned}$$

Under the measure  $\bar{\mathbb{P}}$ , the dynamics are:

$$\begin{aligned} dX_t &= AX_t dt + dM_t \\ dy_t &= dw_t. \end{aligned}$$

Suppose we have an  $\mathbb{F}$ -adapted process given by  $\psi = \{\psi_t : 0 \leq t \leq T\}$ , and let  $\hat{\psi} = \{\hat{\psi}_t : 0 \leq t \leq T\}$  be the  $\mathbb{Y}$ -optional projection of the process  $\psi$ . Under  $\mathbb{P}$ ,  $\hat{\psi}_t = E[\psi_t | \mathcal{Y}_t]$ ,  $\mathbb{P}$ -a.s. Let  $\sigma(\psi) = \{\sigma(\psi_t) : 0 \leq t \leq T\}$  be the  $\mathbb{Y}$ -optional

projection of the process  $\psi\Lambda$  under the measure  $\bar{\mathbb{P}}$ . That is  $\sigma(\psi_t) = \bar{E}[\psi_t|\mathcal{Y}_t]$ ,  $\bar{\mathbb{P}}$ -a.s.

**Definition 4.2.1.** 1. The  $\mathbb{Y}$ -optional projection process  $\hat{\psi}$  is called the normalized filter of  $\psi$ .

2. The process  $\sigma(\psi_t)$  is called unnormalized filter of  $\psi$ .

With using Bayes' rule, we have that

$$\hat{\psi}_t = \frac{\sigma(\psi_t)}{\sigma(1)} \quad \bar{\mathbb{P}}\text{-a.s.} \quad (4.27)$$

where  $\bar{\Lambda}_t = \sigma(1) = \bar{E}[\Lambda_t|\mathcal{Y}_t]$ .

To obtain the dynamics of unnormalized filters, we first need  $\bar{\Lambda}$ .

**Corollary 4.2.1.1.**  $\bar{\Lambda}_t$  is of the form

$$\bar{\Lambda}_t = 1 + \int_0^t \bar{\Lambda}_r \kappa(\langle X_r, g \rangle - y_r) dr. \quad (4.28)$$

*Proof.*  $\bar{\Lambda}_t$  is a  $(\bar{\mathbb{P}}, \mathbb{F})$  martingale. Then, we apply Theorem 4.2.1 with  $H_t = \bar{\Lambda}_r$ ,  $\alpha_r = 0$ ,  $\beta_r = 0$ ,  $\gamma_r = \bar{\Lambda}_r \langle X_r, g \rangle$  and  $y$  is a Brownian motion. Applying Bayes' formula in (4.27), we have the result.  $\square$

Now, we are ready to derive the unnormalized filters. Note that following result is given in [28] without the proof.

**Theorem 4.2.2.** (Theorem 1 in [28]) The recursive equation for the evolution of  $\sigma(HX)$  is given by

$$\begin{aligned} \sigma(H_t X_t) = & \sigma(H_0 X_0) + \int_0^t \sigma(\alpha_r X_{r-}) dr + \int_0^t A_r H_r X_r dr \\ & + \sum_{i,j=1}^n \int_0^t \langle \sigma(\beta_r^j X_{r-} - \beta_r^i X_{r-}), e_i \rangle (a^{ji})_r dr (e_j - e_i) \\ & + \int_0^t (\kappa B_r \sigma(H_{r-} X_r) + \sigma(\delta_r X_{r-})) dy_r \end{aligned}$$

for  $0 \leq t \leq T$ , where  $B_r$  is the  $k \times k$  diagonal matrix with  $B_r = g^i - y_r$ .

*Proof.* From Bayes formula,  $\sigma(H_t X_t) = \bar{\Lambda}_t \widehat{H}_t \widehat{X}_t$ , applying Ito's product rule

$$\begin{aligned} \sigma(H_t X_t) &= \sigma(H_0 X_0) + \int_0^t \sigma(\alpha_r X_r) dr + \int_0^t A H_r X_r dr \\ &\quad + \sum_{i,j=1}^n \int_0^t \langle \sigma(\beta_r^j X_r - \beta_r^i X_r), e_i \rangle (a^{ji})_r dr (e_j - e_i) \\ &\quad + \int_0^t (\sigma(\delta_r X_r) + \kappa B_r \sigma(H_r X_r) - \kappa (\langle \hat{X}_r, g \rangle - y_r) \sigma(H_r X_r)) dw_r \\ &\quad + \int_0^t \kappa (\langle \hat{X}_r, g \rangle - y_r) \sigma(H_r X_r) dy_r + \int_0^t (\kappa (\langle \hat{X}_r, g \rangle - y_r) \sigma(H \delta_r X_r) \\ &\quad + \kappa^2 B_r (\langle \hat{X}_r, g \rangle - y_r) \sigma(H_r X_r) - \kappa^2 (\langle \hat{X}_r, g \rangle - y_r)^2 \sigma(H_r X_r)) dr. \end{aligned}$$

where  $dw_r = dy_r - \int_0^t (\kappa (\langle \hat{X}_r, g \rangle - y_r) dr)$ , replacing  $dw_r$  and after cancellations we get the result.  $\square$

Now, one can obtain the filters for the process  $X$ ,  $N^{ij}$ ,  $J^i$ ,  $G^i$  and  $I^i$  by applying Theorem 4.2.2. First, take  $H_t = H_0 = 1$  and  $\alpha = \beta = \delta = 0$  in Theorem 4.2.2, the recursive filter  $\sigma(X_t)$  for the state process is given by (see also Equation (16) in [29]):

$$\sigma(X_t) = \sigma(X_0) + \int_0^t A_r \sigma(X_r) dr + \int_0^t \kappa B_r \sigma(X_r) dy_r. \quad (4.29)$$

Let  $\mathbf{1} = (1, \dots, 1)$ , then  $\langle X_t, \mathbf{1} \rangle = 1$ . Then, the normalized filter for the state process  $X$  is given by

$$E[X_t | \mathcal{Y}_t] = \hat{X}_t = \frac{\sigma(X_t)}{\langle \sigma(X_t), \mathbf{1} \rangle}.$$

Next, in order to obtain the filters for  $N^{ij}$ , we notice that  $\langle X_{r-}, e_i \rangle X_r = \langle X_{r-}, e_i \rangle e_i$  and thus

$$\sum_{i,j=1}^n \langle \sigma(\beta_r^j X_r - \beta_r^i X_r), e_i \rangle a^{ji} (e_j - e_i) = \langle \langle X_{r-}, e_i \rangle e_i, e_i \rangle a^{ji} (e_j - e_i) + \langle X_{r-}, e_i \rangle a^{ji} (e_j - e_i)$$

Then taking  $H_t = N_t^{ij}$ ,  $H_0 = 0$ ,  $\alpha_r = \langle X_{r-}, e_i \rangle a^{ji}$ ,  $\delta_r = 0$  and  $\beta_r = \langle X_{r-}, e_i \rangle e_j$  in Theorem 4.2.2 and the recursive algorithm  $\sigma(N_t^{ij} X_t)$  for the process  $(N_t^{ij} X_t)$  is (see also Equation (43) in [28]):

$$\sigma(N_t^{ij} X_t) = \int_0^t a^{ji} \langle \sigma(X_r), e_i \rangle e_j dr + \int_0^t A_r \sigma(N_r^{ij} X_r) dr + \int_0^t \kappa B_r \sigma(N_r^{ij} X_r) dy_r.$$

The unnormalized filter for  $N_t^{ij}$  is given as

$$\sigma(N_t^{ij}) = \langle \sigma(N_t^{ij} X_t), \mathbf{1} \rangle,$$



and the normalized filter of  $N_t^{ij}$  is given by

$$E[N_t^{ij}|\mathcal{Y}_t] = \hat{N}_t^{ij} = \frac{\sigma(N_t^{ij})}{\langle \sigma(X_t), \mathbf{1} \rangle}.$$

To get the filter for  $J^i$ , notice that  $\langle X_{r-}, e_i \rangle X_r = \langle X_{r-}, e_i \rangle e_i$ , then apply Theorem 4.2.2 with  $H_t = J_t$ ,  $H_0 = 0$ ,  $\delta_r = \beta_r = 0$ , the recursive filter  $\sigma(J_t^i X_t)$  of the process  $J_t^i X_t$  is

$$\sigma(J_t^i X_t) = \int_0^t \langle \sigma(X_r), e_i \rangle e_i dr + \int_0^t A_r \sigma(J_r^i X_r) dr + \int_0^t \kappa B_r \sigma(J_r^i X_r) dy_r. \quad (4.30)$$

The unnormalized filter for  $J_t^i$  is

$$\sigma(J_t^i) = \langle \sigma(J_t^i X_t), \mathbf{1} \rangle,$$

and the normalized filter  $J_t^i$  is given as

$$E[J_t^i|\mathcal{Y}_t] = \hat{J}_t^i = \frac{\sigma(J_t^i)}{\langle \sigma(X_t), \mathbf{1} \rangle}.$$

Now, applying Theorem 4.2.2 with  $H_t = G_t^i$ ,  $H_0 = 0$ ,  $\delta_r = \kappa(g^i - y_r)\langle X_r, e_i \rangle$ , and  $\beta_r = 0$ , we obtain the recursive algorithm  $\sigma(G_t^i X_t)$  for the process  $G_t^i X_t$  is (see also Equation (47) in [28]):

$$\sigma(G_t^i X_t) = \int_0^t \langle \kappa(g^i - y_r)\sigma(X_r), e_i \rangle e_i dr + \int_0^t A_r \sigma(G_r^i X_r) dr \quad (4.31)$$

$$+ \int_0^t (\kappa B_r \sigma(G_r^i X_r) + \langle \sigma(X_r), e_i \rangle e_i) dy_r. \quad (4.32)$$

The unnormalized filter for  $G_t^i$  is given as

$$\sigma(G_t^i) = \langle \sigma(G_t^i X_t), \mathbf{1} \rangle,$$

and the normalized filter  $G_t^i$  is given as

$$E[G_t^i|\mathcal{Y}_t] = \hat{G}_t^i = \frac{\sigma(G_t^i)}{\langle \sigma(X_t), \mathbf{1} \rangle}.$$

Finally, applying Theorem 4.2.2 with  $H_t = I_t$ ,  $H_0 = 0$ ,  $\alpha_r = y_r \langle X_{r-}, e_i \rangle$ ,  $\delta_r = \beta_r = 0$ , we obtain the recursive algorithm  $\sigma(I_t^i X_t)$  for the process  $I_t^i X_t$  is (see also Equation (50) in [28]):

$$\sigma(I_t^i X_t) = \int_0^t y_r \langle \sigma(X_r), e_i \rangle e_i dr + \int_0^t A_r \sigma(I_r^i X_r) dr + \int_0^t \kappa B_r \sigma(I_r^i X_r) dy_r. \quad (4.33)$$

The unnormalized filter for  $I_t^i$  is given as

$$\sigma(I_t^i) = \langle \sigma(I_t^i X_t), \mathbf{1} \rangle,$$

and the normalized filter  $I_t^i$  is given as

$$E[I_t^i | \mathcal{Y}_t] = \hat{I}_t^i = \frac{\sigma(I_t^i)}{\langle \sigma(X_t), \mathbf{1} \rangle}.$$

#### 4.2.2 Robust Filters

In this part, we aim to derive robust versions of the filters given in Section (4.2.1) using the techniques in [17] and [42]. Using the robust form of a filter instead of the standard form has the advantage of involving minimum number of stochastic integrals compared to the latter case. This yields the corresponding robust discretization of the model. The derived robust filters are not only needed for the robust discretization, but also help us to estimate the volatility of the liquidity within the EM algorithm.

To do this, we consider a diagonal matrix  $\Phi_t$  with entries  $\phi_t^i$  for each  $i$ ,  $1 \leq i \leq K$ . This means that, given

$$\Phi_t = \text{diag}(\phi_t^1, \dots, \phi_t^K)$$

and let define  $B_t = \text{diag}(\langle g, e_i \rangle - y_t)$ ,  $\Phi_t$  has dynamics

$$\Phi_t = \exp(\kappa B_t y_t - \frac{1}{2} \kappa^2 B_t^2 t).$$

It satisfies the following equation

$$d\Phi_t = \Phi_t \kappa B_t dy_t.$$

As a result, the matrix  $\Phi_t$  is invertible and its inverse exists with dynamics:

$$\Phi_t^{-1} = \Phi_0^{-1} - \int_0^t \Phi_r^{-1} \kappa B_r dy_r + \int_0^t \Phi_r^{-1} \kappa^2 B_r^2 dr.$$

For any  $\mathcal{F}$ -adapted, integrable process  $H$  we define the transformation

$$\bar{\sigma}(H_t X_t) = \Phi_t^{-1} \sigma(H_t X_t),$$

where  $\sigma(\cdot)$  indicates the unnormalized filter for  $HX$ .

**Theorem 4.2.3.** *The unnormalized filter  $\sigma(X_t)$  of the state process  $X$  has a robust version defined as*

$$\bar{\sigma}(X_t) = \Phi_t^{-1}\sigma(X_t), \quad \bar{\sigma}(X_0) = \sigma(X_0)$$

*which is a finite variation process and solves the linear ordinary differential equation (ODE) in  $\mathbb{R}^K$ :*

$$\frac{d}{dt}\bar{\sigma}(X_t) = \Phi_t^{-1}A\Phi_t\bar{\sigma}(X_t), \quad \bar{\sigma}(X_0) = \sigma(X_0). \quad (4.34)$$

*Proof.* Apply Ito's product rule to the product  $\Phi_t^{-1}\sigma(X_t)$ .

$$\begin{aligned} d\bar{\sigma}(X_t) &= d\Phi_t^{-1}\sigma(X_t) \\ &= \Phi_t^{-1}d\sigma(X_t) + d\Phi_t^{-1}\sigma(X_t) + [\Phi_t^{-1}, \sigma(X)]_t \\ &= \Phi_t^{-1}A\sigma(X_t)dt + \kappa B_t\Phi_t^{-1}\sigma(X_t)dy_t - \kappa B_t\Phi_t^{-1}\sigma(X_t)dy_t \\ &\quad + \kappa^2 B_t^2\Phi_t^{-1}\sigma(X_t)dt - \kappa^2 B_t^2\Phi_t^{-1}\sigma(X_t)dt \\ &= \Phi_t^{-1}A\sigma(X_t), \end{aligned}$$

with replacing  $\sigma(X_t) = \Phi_t\bar{\sigma}(X_t)$

$$\bar{\sigma}(X_t) = \Phi_t^{-1}A\Phi_t\bar{\sigma}(X_t)dt.$$

□

**Corollary 4.2.3.1.** *The solution of the unnormalized filter of the state process  $X$  is given by*

$$\sigma(X_t) = \Phi_t\bar{\sigma}(X_t) \quad (4.35)$$

where

$$\sigma(X_t) = \sigma(X_0) + \int_0^t A_r\sigma(X_r)dr + \int_0^t \kappa B_r\sigma(X_r)dy_r.$$

*Proof.* Apply Ito's product rule to the product  $\Phi_t\bar{\sigma}(X_t)$ .

$$\begin{aligned} d\sigma(X_t) &= d\Phi_t\bar{\sigma}(X_t) \\ &= \Phi_t d\bar{\sigma}(X_t) + d(\Phi_t)\bar{\sigma}(X_t) + [\Phi, \bar{\sigma}(X_t)]_t \\ &= \Phi_t\Phi_t^{-1}A\Phi_t\bar{\sigma}(X_t)dt + \Phi_t\kappa B_tdy_t\bar{\sigma}(X_t)dt \\ &= A\sigma(X_t)dt + \kappa B_t\sigma(X_t)dy_t \\ \sigma(X_t) &= \sigma(X_0) + \int_0^t A_r\sigma(X_r)dr + \int_0^t \kappa B_r\sigma(X_r)dy_r. \end{aligned}$$

□

In the same vein, using the process  $\Phi_t^{-1}$  the robust filters can be obtained for the other quantities.

**Proposition 4.2.3.1.** 1. *The recursive nonlinear stochastic integral equation has a robust version, i.e.  $\bar{\sigma}(N_t^{ij} X_t) = \Phi_t^{-1} \sigma(N_t^{ij} X_t)$  that satisfies the following equation*

$$\bar{\sigma}(N_t^{ij} X_t) = \int_0^t \langle \bar{\sigma}(X_r), e_i \rangle a^{ji} e_j dr + \int_0^t \Phi_r^{-1} A \Phi_r \bar{\sigma}(N_r^{ij} X_r) dr \quad (4.36)$$

with initial condition  $\bar{\sigma}(N_0^{ij} X_0) = 0$ .

2. *The recursive nonlinear stochastic integral equation has a robust version, i.e.  $\bar{\sigma}(J_t^i X_t) = \Phi_t^{-1} \sigma(J_t^i X_t)$  that satisfies the following equation*

$$\bar{\sigma}(J_t^i X_t) = \int_0^t \langle \bar{\sigma}(X_r), e_i \rangle e_i dr + \int_0^t \Phi_r^{-1} A \Phi_r \bar{\sigma}(J_r^i X_r) dr \quad (4.37)$$

with initial condition  $\bar{\sigma}(J_0^i X_0) = 0$ .

3. *The recursive nonlinear stochastic integral equation has a robust version, i.e.  $\bar{\sigma}(G_t^i X_t) = \Phi_t^{-1} \sigma(G_t^i X_t)$  that satisfies the following equation*

$$\bar{\sigma}(G_t^i X_t) = \int_0^t \langle \bar{\sigma}(X_r), e_i \rangle e_i dy_r + \int_0^t \Phi_r^{-1} A \Phi_r \bar{\sigma}(G_r^i X_r) dr \quad (4.38)$$

with initial condition  $\bar{\sigma}(G_0^i X_0) = 0$ .

4. *The recursive nonlinear stochastic integral equation has a robust version, i.e.  $\bar{\sigma}(I_t^i X_t) = \Phi_t^{-1} \sigma(I_t^i X_t)$  that satisfies the following equation*

$$\bar{\sigma}(I_t^i X_t) = \int_0^t y_r \langle \bar{\sigma}(X_r), e_i \rangle e_i dr + \int_0^t \Phi_r^{-1} A \Phi_r \bar{\sigma}(I_r^i X_r) dr \quad (4.39)$$

with initial condition  $\bar{\sigma}(I_0^i X_0) = 0$ .

*Proof.* Proofs of (4.36) to (4.39) in (4.2.3.1) are obtained by applying Ito's product formula to  $\Phi_t^{-1} \sigma(N_t^{ij} X_t)$ ,  $\Phi_t^{-1} \sigma(J_t^i X_t)$ ,  $\Phi_t^{-1} \sigma(G_t^i X_t)$  and  $\Phi_t^{-1} \sigma(I_t^i X_t)$  respectively and are very similar to proof of Theorem 4.2.3. Thus, they are omitted.  $\square$

Furthermore, it can be shown that  $\Phi_t \bar{\sigma}(N_t^{ij} X_t)$ ,  $\Phi_t \bar{\sigma}(J_t^i X_t)$ ,  $\Phi_t \bar{\sigma}(G_t^i X_t)$  and  $\Phi_t \bar{\sigma}(I_t^i X_t)$  are the solutions of  $\sigma(N_t^{ij} X_t)$ ,  $\sigma(J_t^i X_t)$ ,  $\sigma(G_t^i X_t)$  and  $\sigma(I_t^i X_t)$ , respectively. Proofs are very similar to the proof of Corollary (4.2.3.1) and thus they are omitted.

#### 4.2.2.1 Discrete time filters

To perform numerical computation, the equation needs to be discretized in time. There are two approaches to do this: one approach is to directly discretize the continuous-time filters presented in Section (4.2.2). The other approach is to discretize the robust filters. The following will explain the process of discretizing the robust filters. Consider a constant time step  $\Delta = t_n - t_{n-1}$  and take the ODE (4.34):

$$\begin{aligned}\bar{\sigma}(X_{t_n}) &= \bar{\sigma}(X_{t_{n-1}}) + \int_{t_{n-1}}^{t_n} \Phi_s^{-1} A \Phi_s \bar{\sigma}(X_s) ds \\ &\simeq \bar{\sigma}(X_{t_{n-1}}) + \Phi_{t_{n-1}}^{-1} A \Phi_{t_{n-1}} \bar{\sigma}(X_{n-1}) \Delta \\ &\simeq [I + \Phi_{t_{n-1}}^{-1} A \Phi_{t_{n-1}}] \bar{p}_{t_{n-1}},\end{aligned}\tag{4.40}$$

which gives the following explicit approximation

$$\bar{\sigma}(X_n) = [I + \Phi_{t_{n-1}}^{-1} A \Phi_{t_{n-1}}] \bar{\sigma}(X_{n-1}).\tag{4.41}$$

Multiplying both sides by  $\Phi_{t_n}$  gives the following approximation

$$\sigma(X_n) = \Phi_{t_n} \Phi_{t_{n-1}}^{-1} [I + \Delta A] \sigma(X_{n-1}) = \Psi_n [I + \Delta A] \sigma(X_{n-1})\tag{4.42}$$

where

$$\Psi_t^s = \Phi_t \Phi_s^{-1} = \exp(\kappa B_{t-1} (y_t - y_{t-1}) - \frac{1}{2} \kappa^2 B_{t-1}^2 dt)$$

and

$$\Psi_n = \Phi_{t_n} \Phi_{t_{n-1}}^{-1} = \text{diag}(\psi_n^1, \dots, \psi_n^N) \quad \text{with} \quad \psi_n^i = \phi_{t_n}^i / \phi_{t_{n-1}}^i.$$

The equation given in (4.42) is a discrete time approximation for the Duncan-Mortensen-Zakai equation.

For a small enough time step  $\Delta = t_n - t_{n-1}$ , denote the generator matrix by  $A^*$ ,  $P = [I + \Delta A^*]$  is the transition probability matrix with entries  $\pi_{ij}$ , then we define the fast sample observations

$$z_n^\Delta = \frac{1}{\Delta} [y_{t_n} - y_{t_{n-1}}], \quad n = 1, 2, \dots, N.$$

Now, we can work under the discrete hidden Markov model setting. Our discrete time model becomes as following

$$z_n^\Delta = \kappa(g(X_n) - Y_{t_n}) + W_n^\Delta\tag{4.43}$$

where  $(X_n)_{(n \geq 0)}$  is a discrete-time Markov chain with a state space  $S = \{e_1, \dots, e_K\}$  and  $\{(W_n^\Delta)_{(n \geq 0)}\}$  is a Gaussian white noise sequence with a covariance matrix  $\Delta^{-1}I$ . Let us write

$$F_n = \sigma(X_n, z_n^\Delta, 0 \leq n \leq N)$$

and

$$Y_n = \sigma(z_n^\Delta, 0 \leq n \leq N).$$

The EM algorithm for the introduced discrete time model requires the conditional expectations of the following quantities:

- i)  $X_n$ , state of the Markov chain.
- ii)  $N_n^{ij}$ , the number of transitions of the Markov chain from the state  $e_i$  to the state  $e_j$  up to time  $N$

$$N_n^{ij} = \sum_{n=1}^N \langle X_{n-1}, e_i \rangle \langle X_n, e_j \rangle. \quad (4.44)$$

- iii)  $J_n^i$ , the occupation visit of the process  $X$  in state  $e_i$  until time  $N$

$$J_n^i = \sum_{n=1}^N \langle X_{n-1}, e_i \rangle. \quad (4.45)$$

- iv)  $G_n^i$ , the level sum in the state  $e_i$  until time  $N$

$$G_n^i = \sum_{n=1}^N \langle X_{n-1}, e_i \rangle z_n^\Delta. \quad (4.46)$$

- v)  $I_n^i$ , the auxiliary process in state  $e_i$  up to time  $N$

$$I_n^i = \sum_{n=1}^N y_n \langle X_{n-1}, e_i \rangle. \quad (4.47)$$

In the same vein, to obtain discrete time unnormalized filters, we first discretize the robust filters in from 4.36 to 4.39 by Euler Maruyama scheme. Then we multiply both sides of the equations with  $\Phi_{t_n}$ . The discrete time unnormalized filters are given

as:

$$\sigma(N_n^{ij} X_n) = \Psi_n P^* \sigma(N_{n-1}^{ij} X_{n-1}) + \langle \sigma(X_{n-1}), e_i \rangle \langle \Psi_n P^* e_i, e_j \rangle e_j \quad (4.48)$$

$$\sigma(J_n^i X_n) = \Psi_n P^* \sigma(J_{n-1}^i X_{n-1}) + \langle \sigma(X_{n-1}), e_i \rangle \Psi_n P^* e_i \quad (4.49)$$

$$\sigma(G_n^i X_n) = \Psi_n P^* \sigma(G_{n-1}^i X_{n-1}) + z_n^\Delta \langle \sigma(X_{n-1}), e_i \rangle \Psi_n P^* e_i \quad (4.50)$$

$$\sigma(I_n^i X_n) = \Psi_n P^* \sigma(I_{n-1}^i X_{n-1}) + Y_{n-1} \langle \sigma(X_{n-1}), e_i \rangle \Psi_n P^* e_i. \quad (4.51)$$

**Remark 4.2.1.** *If the log likelihood function for the discrete time model is a good approximation to the likelihood function for the continuous time model, then the parameter estimates obtained from the maximization step in the discrete time setting should be reasonably close to a stationary point of the likelihood function for the continuous time model. In other words, if the discrete time model provides a good representation of the underlying continuous time dynamics, the estimates obtained from the discrete time optimization procedure should align with the maximum likelihood estimates of the continuous time model.*

This assumption relies on the idea that as the time interval between observations in the discrete time model becomes infinitesimally small, the discrete time model approaches the continuous time model. Therefore, if the discrete time model accurately captures the essential features of the continuous time process, the parameter estimates obtained from the discrete time estimation should be close to the stationary point of the continuous time likelihood function.

However, it is important to note that this assumption depends on the specific modeling framework, the nature of the data, and the underlying assumptions of the continuous time model. Careful validation and testing of the approximation and parameter estimates are necessary to ensure the reliability and accuracy of the results.

Based on Remark (4.2.1), now, we can work under the discrete hidden Markov model setting.

To avoid numerical overflows, we normalize the filters in (4.40) and (4.48) to (4.51). First, we define the normalization constant  $c_n = \langle \Psi_n P^* \sigma(X_{n-1}), \mathbf{1} \rangle$ .

Take  $H_n = N_n^{ij}, J_n^i, G_n^i$  and  $I_n^i$ , we define

$$\widehat{H_n X_n} = \sigma(H_n X_n) / \gamma_n$$

where

$$\gamma_n = \langle \sigma(X_n), \mathbf{1} \rangle = c_n \cdot c_{n-1} \cdots c_1.$$

The normalized discrete time recursive filters are:

$$\sigma(X_n) = \Psi_n P^* \sigma(X_{n-1}) / c_n \quad (4.52)$$

$$\sigma(N_n^{ij} X_n) = [\Psi_n P^* \sigma(N_{n-1}^{ij} X_{n-1}) + \langle \sigma(X_{n-1}), e_i \rangle \langle \Psi_n P^* e_i, e_j \rangle] / c_n \quad (4.53)$$

$$\sigma(J_n^i X_n) = [\Psi_n P^* \sigma(J_{n-1}^i X_{n-1}) + \langle \sigma(X_{n-1}), e_i \rangle \Psi_n P^* e_i] / c_n \quad (4.54)$$

$$\sigma(G_n^i X_n) = [\Psi_n P^* \sigma(G_{n-1}^i X_{n-1}) + z_n^\Delta \langle \sigma(X_{n-1}), e_i \rangle \Psi_n P^* e_i] / c_n \quad (4.55)$$

$$\sigma(I_n^i X_n) = [\Psi_n P^* \sigma(I_{n-1}^i X_{n-1}) + y_{n-1} \langle \sigma(X_{n-1}), e_i \rangle \Psi_n P^* e_i] / c_n. \quad (4.56)$$

#### 4.2.2.2 Variance Estimation

The filtering procedure introduced by [29] utilizes the change of measure technique, however, it does not provide an MLE for the noise variance as the corresponding measures with different variances for the diffusion process are not absolutely continuous [42]. In [29], the filtering equations are derived under the assumption of known variance by scaling the process accordingly. In real-world scenarios, the noise variance is not known. On the other hand, [42] explains how to obtain the MLE of the noise variance in a robust filtering setting. Similarly, we provide the ML estimate of the noise variance of the model in the EM algorithm.

Denote by  $\varsigma^2$  the noise variance, then the process in (4.43), has a variance  $\varsigma^2 / \Delta$ . Including  $\varsigma$  as a new parameter to be estimated, our new parameter set becomes  $\theta^* = (a^{*ij}, g^{*i}, \kappa^*, \varsigma^*, 1 \leq i, j \leq K)$  with the corresponding probability measure  $\mathbb{P}^*$  and the updated parameter set is  $\theta = \{a^{ij}, g^i, \kappa, \varsigma, 1 \leq i, j \leq K\}$  with respective probability measure  $\mathbb{P}_\theta$ . Then consider the Radon-Nikodym derivative  $\frac{d\mathbb{P}_\theta}{d\mathbb{P}_{\theta^*}}$ , we have the likelihood ratio:

$$\frac{d\mathbb{P}_\theta}{d\mathbb{P}_{\theta^*}} = \prod_{n=1}^N \frac{\frac{1}{\sqrt{2\pi\varsigma^2/\Delta}} \exp\left(-\frac{|z_n^\Delta - \kappa(\langle g, X_{n-1} \rangle - y_{n-1})|^2}{2\varsigma^2/\Delta}\right)}{\frac{1}{\sqrt{2\pi\varsigma^{*2}/\Delta}} \exp\left(-\frac{|z_n^\Delta - \kappa^*(\langle g^*, X_{n-1} \rangle - y_{n-1})|^2}{2\varsigma^{*2}/\Delta}\right)}.$$



The filtered log-likelihood of the discrete time model can be written as:

$$\begin{aligned} \widehat{L}(\theta, \theta^*) &= E \left[ \log \frac{d\mathbb{P}_\theta}{d\mathbb{P}_{\theta^*}} | \mathcal{Y}_n \right] = -\frac{N}{2} \log \left( \frac{\zeta^2}{\Delta} \right) \\ &\quad + \frac{\zeta^2}{\Delta} \left( |z_n^\Delta|^2 - 2|z_n^\Delta| \kappa g \langle X_{n-1}, e_i \rangle + 2\kappa z_n^\Delta y_{n-1} \right. \\ &\quad \left. + \kappa^2 g^2 \langle X_{n-1}, e_i \rangle - 2\kappa^2 g \langle X_{n-1}, e_i \rangle y_{n-1} + \kappa^2 y_{n-1}^2 \right) + \hat{R}(\theta^*), \end{aligned} \quad (4.57)$$

where  $\hat{R}(\theta^*)$  is independent from  $a^{ij}, g^i, \kappa, \zeta$ .

Using Equations from (4.44) to (4.47), note that

$$\begin{aligned} \hat{N}_n^{ij} &= E(N_n^{ij} | \mathcal{Y}_n) = \frac{\langle \sigma(N_n^{ij} X_n), 1 \rangle}{\langle \sigma(X_n), 1 \rangle}, \quad \hat{J}_n^i = E(J_n^i | \mathcal{Y}_n) = \frac{\langle \sigma(J_n^i X_n), 1 \rangle}{\langle \sigma(X_n), 1 \rangle}, \\ \hat{G}_n^i &= E(G_n^i | \mathcal{Y}_n) = \frac{\langle \sigma(G_n^i X_n), 1 \rangle}{\langle \sigma(X_n), 1 \rangle} \quad \text{and} \quad \hat{I}_n^i = E(I_n^i | \mathcal{Y}_n) = \frac{\langle \sigma(I_n^i X_n), 1 \rangle}{\langle \sigma(X_n), 1 \rangle}. \end{aligned}$$

We rewrite (4.57) as

$$\begin{aligned} \widehat{L}(\theta, \theta^*) &= -\frac{N}{2} \log \left( \frac{\zeta^2}{\Delta} \right) \\ &\quad + \frac{\zeta^2}{\Delta} \left( \sum_{i=1}^K (\kappa^2 g^2 \hat{J}_N^i - 2\kappa^2 g \hat{I}_N^i - 2\kappa g \hat{G}_N^i) \right. \\ &\quad \left. + \sum_{n=1}^N |z_n^\Delta|^2 + \kappa^2 y_{n-1}^2 + 2\kappa z_n^\Delta y_{n-1} \right) + \hat{R}(\theta). \end{aligned} \quad (4.58)$$

Maximizing (4.58) with respect to  $\zeta$ , we obtain the following estimate for  $\zeta$ :

$$\begin{aligned} \hat{\zeta}^2 &= -\frac{\Delta}{N} \left( \sum_i^K (\kappa^2 (g^i)^2 (\hat{J}_N^i)^2 - 2\kappa^2 g^i \hat{I}_N^i - 2\kappa g^i \hat{G}_N^i) \right. \\ &\quad \left. + \sum_{n=1}^N |z_n^\Delta|^2 + \kappa^2 |y_{n-1}|^2 + 2\kappa |y_{n-1} z_n^\Delta| \right) \end{aligned}$$

where,  $\hat{\kappa} = \frac{C}{D}$  with

$$C = \sum_i^K |y_{n-1} z_n^\Delta| - \sum_i^K \frac{\hat{I}_N^i \hat{G}_N^i}{\hat{J}_N^i}, \quad D = \sum_i^K \frac{(\hat{I}_N^i)^2}{\hat{J}_N^i} - \sum_n^N |y_{n-1}|^2.$$

and

$$\hat{g}^i = \frac{\hat{\kappa}^{-1} \hat{G}_N^i + \hat{I}_N^i}{\hat{J}_N^i}.$$

The update from  $a^{*ji}$  to  $\hat{a}^{ji}$  does not change and it is:

$$\hat{a}^{ji} = \frac{\hat{N}_N^{ij}}{\hat{J}_N^i}.$$

## CHAPTER 5

### SIMULATION STUDY

#### 5.1 Simulation

In this section, we evaluate the performance of proposed robust filtering methodology with the existing methodology in the literature. More specifically, we compare the cases with robust filters and continuous time filters, which are required in the E-step of the parameter estimation of the OU model. For the numerical application, we discretize the continuous time filters given in (4.2.1) by both Euler and Milstein approaches. As for the robust filters, we use the discrete time recursive filters given in (4.2.2.1). We compare their performances from different aspects. These can be phrased in three questions as follows:

- a) How does the step size affect the performance of the EM algorithm?
- b) How does the drift affect the performance of the EM algorithm?
- c) How does the volatility affect the performance of the EM algorithm?

This examination is essential for refining the methods and establishing a connection between theoretical concepts and their practical implementation.

#### Algorithm

Step 1 We fix a parameter set  $\theta$ , an initial distribution  $\pi$ , some noise variance  $\varsigma$  and

generate trajectories of size  $N$  with step size  $\Delta$  for the Markov chain  $X$  and Brownian motion  $W$ . Then, we obtain the corresponding observation series  $y$ .

Step 2 We run the EM algorithm and obtain estimates for the hidden states, as well as for the parameters following steps:

- i) Initialize the algorithm with some parameter set  $\theta^0$ .
- ii) Normalize the data by  $\varsigma$ .
- iii) Obtain the filtered estimates of the quantities of interest.
- iv) Compute  $\theta^{n+1}$ .
- v) Terminate if  $\frac{|\theta^{n+1} - \theta^n|}{|\theta^n|}$  are below the termination tolerance; else return to step N.

Numerical approximations have been developed with the unavailability of the solutions of SDEs. Usually, these methods rely on time discretization with points  $0 = t_0 < t_1 < \dots < t_n < \dots < t_N = T$  within the time interval  $[0, T]$ , employing a step-size  $\Delta = t_{n+1} - t_n$ .

It is possible to use time discretizations that are not necessarily based on a fixed step-size but could instead be random. However, the research by [18] has demonstrated that not all traditional or heuristic time discretization methods for stochastic differential equations (SDEs) converge meaningfully to the solution process as the step size  $\Delta$  approaches zero. As a result, a systematic approach is necessary to choose an effective and trustworthy numerical method to overcome the problem.

The most widely used time discretization methods of SDEs are Euler-Maruyama method and Milstein method.

**a) Euler-Maruyama discretization:** To obtain numerical solutions for underlying differential equations, we start with Euler-Maruyama discretization, which is also known as naive discretization. This method is based on the first order approximation. As an example, we discretize the stochastic filter  $\sigma(X)$  of the state process of the MC with Euler Maruyama scheme given as:

$$\sigma(X_n) = \sigma(X_{n-1}) + A\sigma(X_{n-1})\Delta + \kappa B_{n-1}\sigma(X_{n-1})(y_n - y_{n-1}). \quad (5.1)$$

**b) Milstein discretization:** The Milstein method is a numerical approximation technique used to solve stochastic differential equations (SDEs) that improve upon the accuracy of the Euler-Maruyama method. The method includes a second-order correction term derived from the stochastic Taylor series expansion of the solution to the given SDE, which is obtained by applying Ito's lemma. This correction term allows for a more accurate approximation of the solution, particularly for SDEs with strong drift and moderate to large diffusion coefficients. To obtain the Milstein method, we need to retain terms up to the second order of the Brownian increment. The differential form of the Milstein method for the stochastic filter  $\sigma(X)$  of the state process of the MC is given by:

$$\begin{aligned} \sigma(X_n) = & \sigma(X_{n-1}) + A\sigma(X_{n-1})\Delta + \kappa B_{n-1}\sigma(X_{n-1})(y_n - y_{n-1}) \\ & + \frac{1}{2}[(y_n - y_{n-1})^2 - \Delta]\kappa^2 B_{n-1}^2\sigma(X_{n-1}). \end{aligned} \quad (5.2)$$

**c) Robust discretization:** We use the discrete time filters that are based on the robust filters discretization. To avoid numerical issues, we use the normalized ones as given in (4.53) to (4.56). Recall the normalized discrete time filter for the state process  $X$

$$\sigma(X_n) = \Psi_n P^* \sigma(X_{n-1}) / c_n. \quad (5.3)$$

We consider a 3-state MC with the parameters listed in Table 5.1.  $N$  represents the number of data points, and  $\Delta$  denotes the step-size.

Table 5.1: Parameters used in the algorithm

$a^{12}$	$a^{13}$	$a^{21}$	$a^{23}$	$a^{31}$	$a^{32}$	$g^1$	$g^2$	$g^3$	$\varsigma$	$\kappa$	$T$	$\Delta$	$N$
0.3	0.4	0.4	0.3	0.3	0.2	-6	0.2	5	2	5	20	1/250	$T/\Delta$

We generate  $N$  number of observations  $y_1, \dots, y_N$  by fixing the parameter set  $\theta$ , initial distribution  $\pi$ , and noise variance  $\varsigma_Y^2$  for the Markov chain  $X$ . We start the algorithm with the initial values equal to the half of the true values and set the tolerance level 0.01. The evolution of the filtered estimate of Markov chain  $X$  can be seen in Figure 5.1.

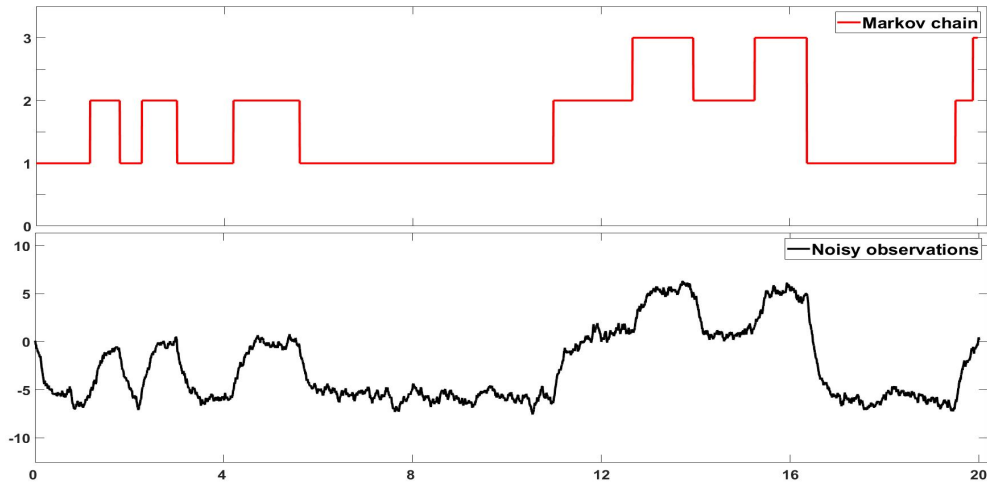


Figure 5.1: Markov chain and noisy observation process

### 5.1.1 How does $\Delta$ affect the performance of the EM algorithm?

In this part, we examine the effect of changes in step size on the EM algorithms. We compare the results for  $\Delta = 1/80$  and  $\Delta = 1/250$ . We assume that the volatility is known and equal to 2. The rest of the parameters used in the simulation is the half of the parameters given in Table 5.1.

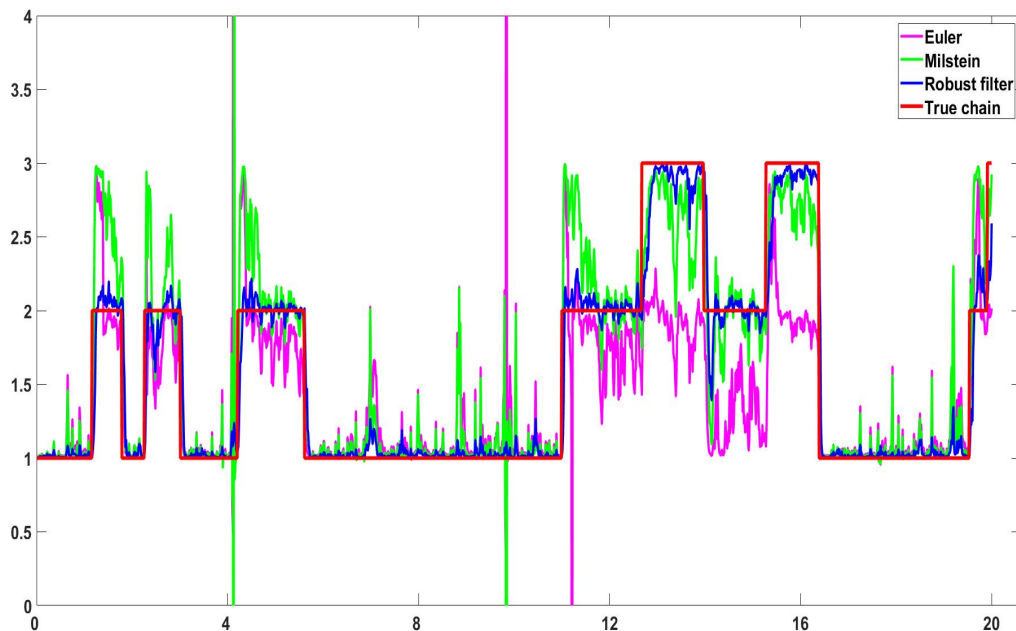


Figure 5.2: EM estimates vs. true chain,  $\Delta = 1/80$

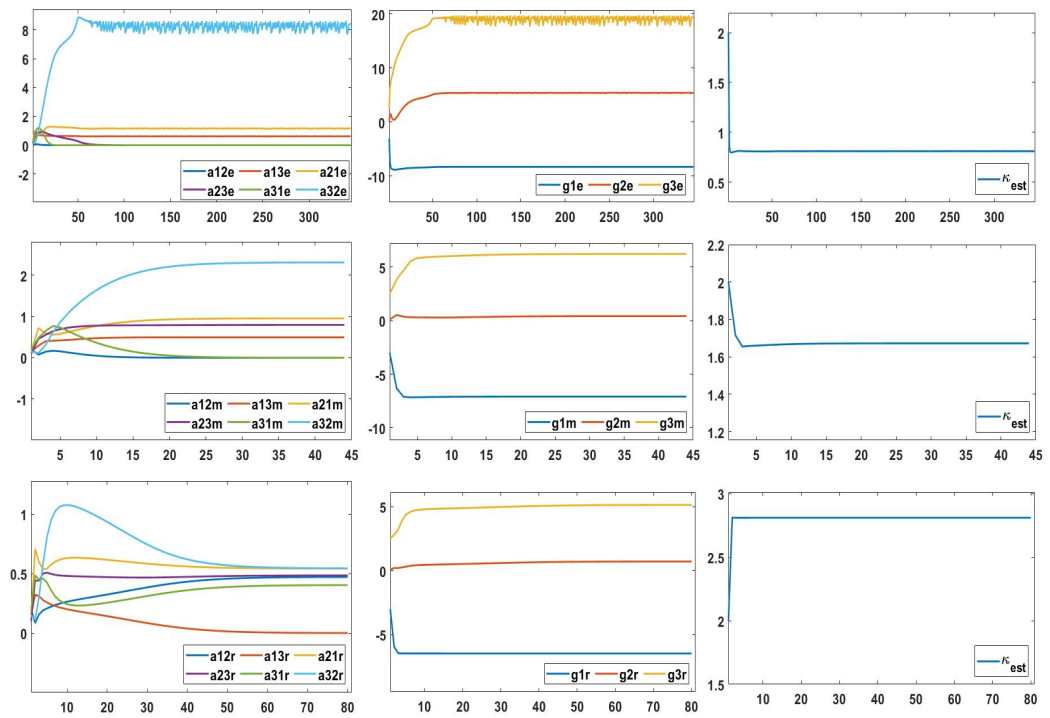


Figure 5.3: Evolution of parameter estimates for  $A$ ,  $g$  and  $\kappa$ ,  $\Delta = 1/80$

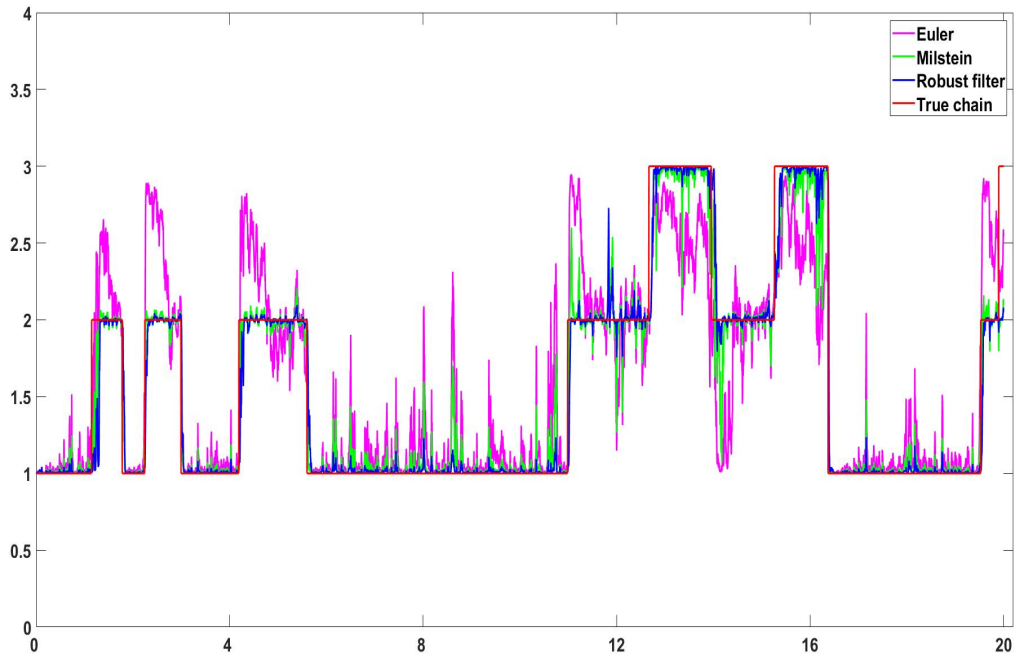


Figure 5.4: EM estimates vs. true chain,  $\Delta = 1/250$

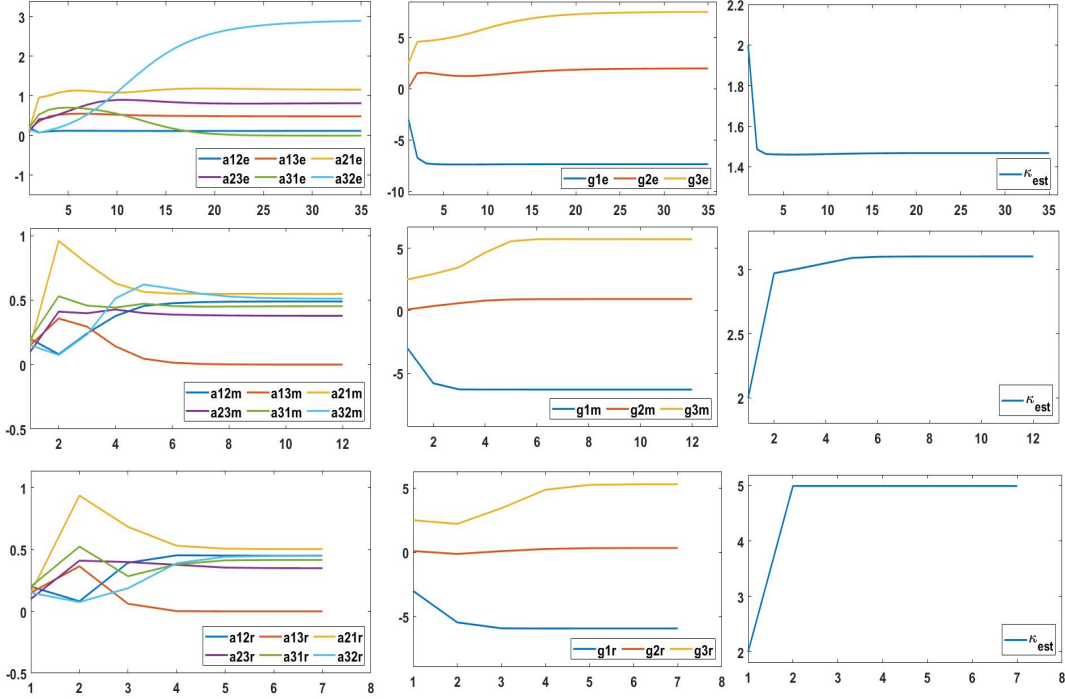


Figure 5.5: Evolution of parameter estimates for  $A$ ,  $g$  and  $\kappa$ ,  $\Delta = 1/250$

Applying different step sizes, the algorithm with robust filters has the best performance among others, by following a clear track to the true chain as seen in Figures 5.2 and 5.4. On the other hand, Euler discretized model shows the worst performance. More specifically, it cannot catch the regime switches in higher step size application and thus, does not give good results in parameter estimates. Discretized robust filter setting shows the best convergence to the true parameter set in parameter estimation results, see Figures 5.3 and 5.5. In general, when we decrease the step size, performance of all models increases and the number of iterations decreases.

### 5.1.2 How does drift (relative to noise variance) affect the performance of the EM algorithm?

In this part, we want to see how drift variations affect the performance of the algorithm with different numerical methods. We use the step size  $\Delta = 1/250$  and assume that the standard deviation is known. We use the same parameter set given in Table 5.1. First, we start with a drift such that it provides a clear trend in the data process as seen in the bottom of Figure 5.1. Then, we make the trend less obvious, i.e. the



drift part is dominated by the noise part, which means that our data process shows flatter process with using drift parameters as  $g = (-1 \ 0.2 \ 1)$ . When data process does not show any clear trend or information and so is dominated by the noise, the EM algorithm with Euler and Milstein approximations have a failure to show reasonable results, see Figure 5.6. On the contrary, the discretized robust filter scheme gives a better result by tracking the true chain and provides closer results in parameter estimates compared to other EM algorithms. In detail, it provides very close result drift estimates to true drift parameters. However, it overestimates the entries of the generator matrix and  $\kappa$  value than true parameters, see Figure 5.7.

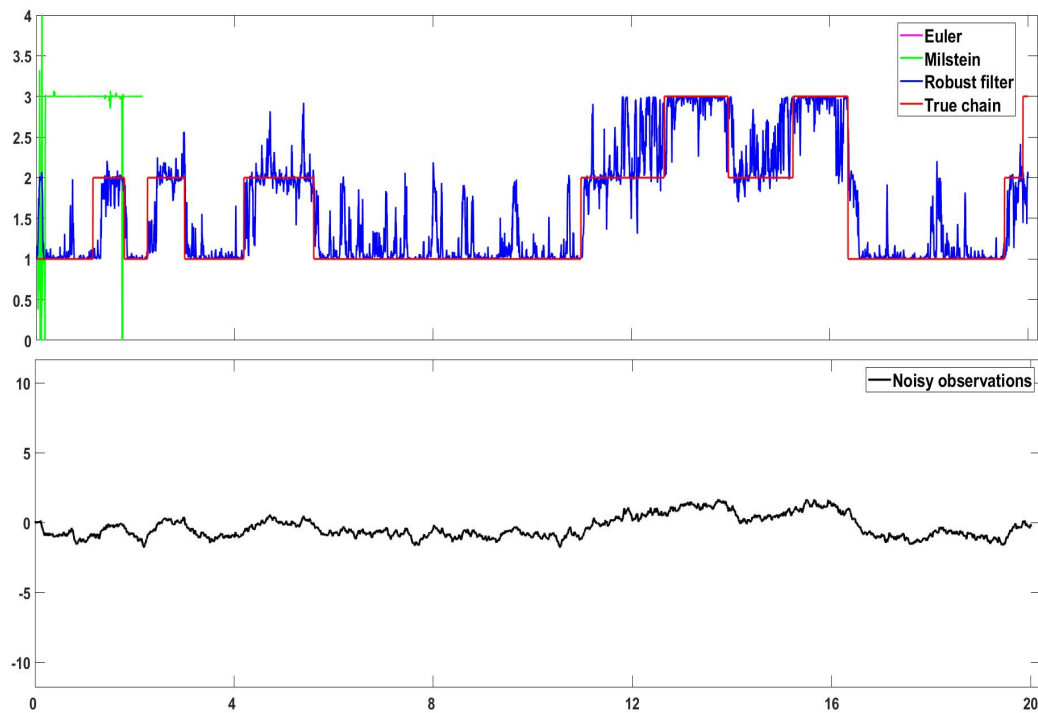


Figure 5.6: EM estimates vs. true chain,  $g = [-1 \ 0.2 \ 1]$

### 5.1.3 How does the noise variance affect the performance of the EM algorithm?

The final performance comparison is based on the noise variance effect. So far, we have assumed that the variance is known and EM algorithm starts with true parameter. Here, we start the EM algorithm with different standard deviation,  $\varsigma = 1$  rather than true standard deviation,  $\varsigma = 2$ . The Figure 5.8 clearly shows the effect of variance estimation. The continuous-time filter with different approximations fails when start-

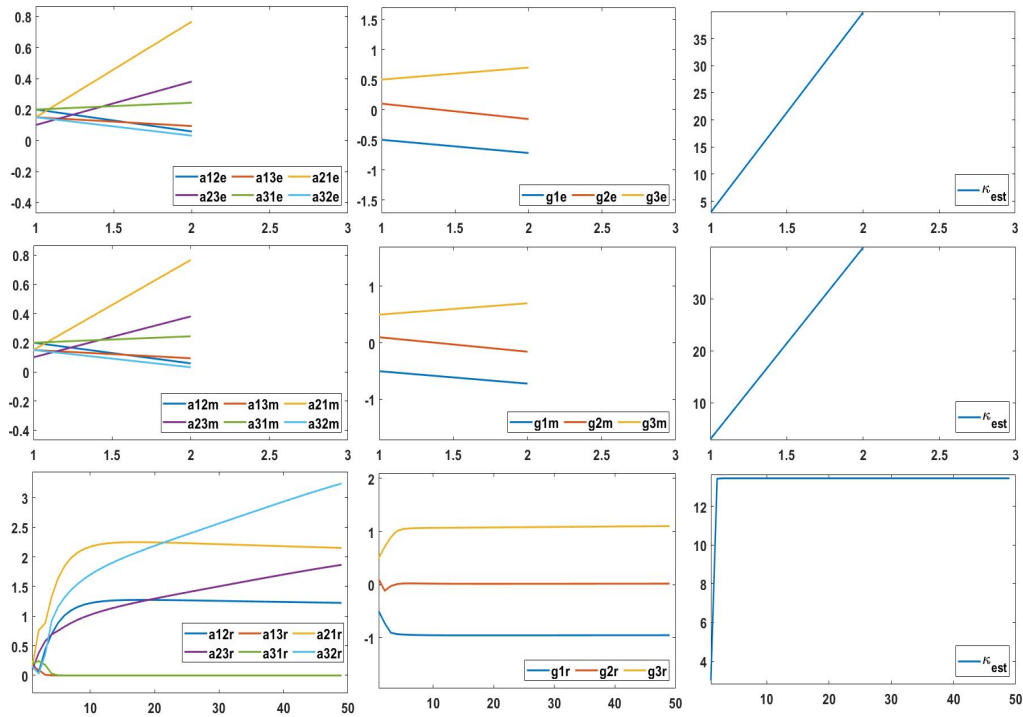


Figure 5.7: Evolution of parameter estimates for  $A$ ,  $g$  and  $\kappa$ ,  $g = [-1 \ 0.2 \ 1]$

ing with different noise variance, while the robust filter performs well and produces results that are very close to the true Markov chain.

The Figure 5.9 shows the evolution of the parameter estimates for  $A$ ,  $g$ ,  $\varsigma$  and  $\kappa$  that are obtained from the robust filters. All parameters exhibit the convergence to the true parameters. The only exception is the final estimate of the volatility which is slightly higher than the true parameter.

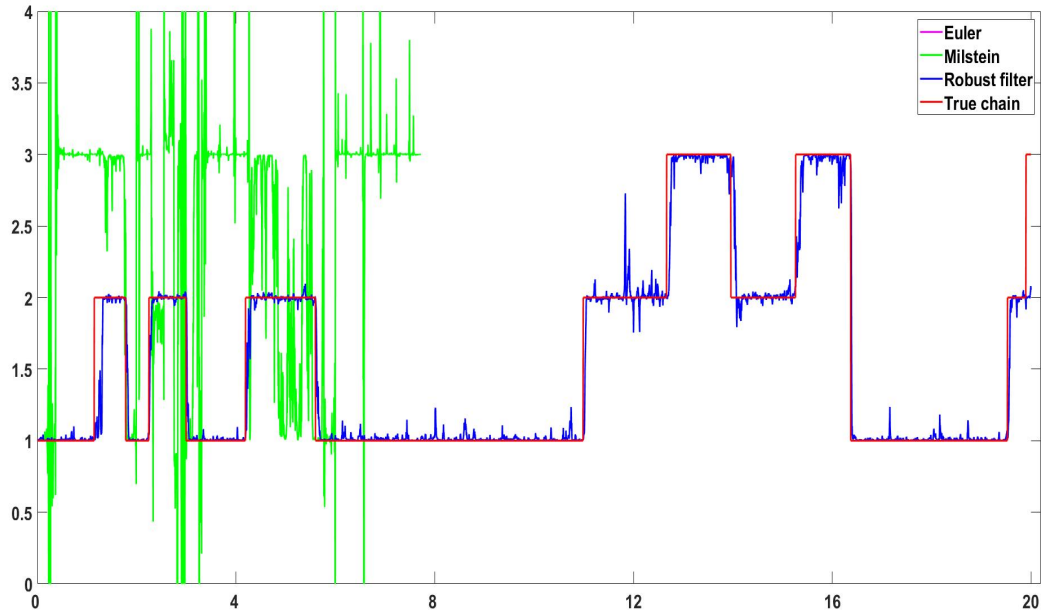


Figure 5.8: EM estimates vs. true chain

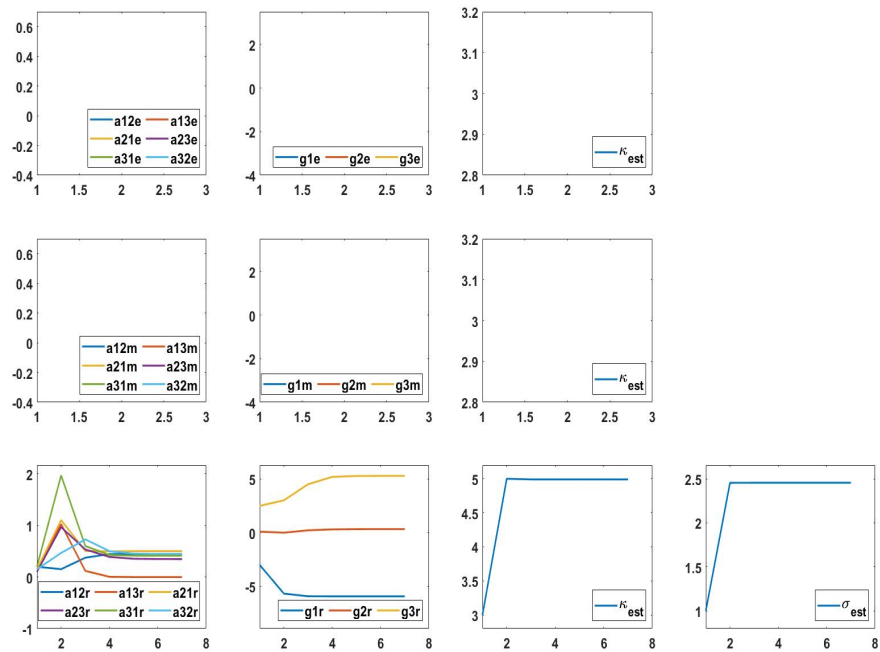


Figure 5.9: Evolution of parameter estimates for  $A$ ,  $g$  and  $\kappa$



## CHAPTER 6

### DATA APPLICATION

In this chapter, a real data set is employed to illustrate the implementation of the proposed model. We assume that the implied liquidity series provide noisy information on the true market liquidity level. Overall, we aim to evaluate the true market liquidity through the use of implied liquidity as a proxy. First, we describe the data and explain how to derive it. After applying our proposed model to the data, we evaluate the results based on in sample and out of sample results. Specifically, the number of states are determined based on using AIC and BIC values in the sample results. In out of sample testing, we evaluate the performance of the proposed model according to point forecast and interval forecast results.

#### 6.1 Data

The data contains the daily bid and ask prices of European call option written on the S&P 500 index in the period from the 1st January 2002 to the 1st August 2022. The data is retrieved from [ivolatility.com](http://ivolatility.com) and it also includes daily value of underlying asset S&P 500 index ([ivolatility.com](http://ivolatility.com)), daily value of 3-month US Treasury bill rate ([fred.stlouis.org](http://fred.stlouis.org)) and daily value of implied volatility ([ivolatility.com](http://ivolatility.com)) for the same period.

We have a large data set of 34,438,878 observations. Following a similar procedure in [1], we produce the implied liquidity series. In the data set, we have daily option prices with various strikes and maturities. Denote by  $n$  the  $n^{\text{th}}$  day of the data period  $n \in 1, \dots, N$ . On each day of the sample period, we choose an option based on two

criteria: (closest to) 1-year ATM call options and the highest trading volume if several options are available the same day after applying the first criteria. After extracting the option series, the goal is to find the implied liquidity parameter  $L_n$  that best matches the theoretical bid, and ask prices with the observed bid, and ask prices at day  $n$ . Accordingly, we obtain the implied liquidity by minimizing the squared error (SE) between the theoretical bid and ask prices  $(a_{L,n}, b_{L,n})$  and the observed market bid and ask prices  $(a_n, b_n)$ . That is, for each day of the sample period, we solve the following minimization problem:

$$\begin{aligned} \min_{L_n} \quad & SE_{bid,ask}(L_n) = (b_n - b_{L,n})^2 + (a_n - a_{L,n})^2 \\ \text{s.t.} \quad & L_n \geq 0. \end{aligned}$$

We repeat this procedure on each day of the data series, and obtain the implied liquidity series. Note that, we multiply the resulting series with 100 to obtain the values in basis points. The the logarithm of the daily implied liquidity series is plotted in Figure 6.1. Following its definition, higher values of implied liquidity correspond to lower liquidity in the underlying market and vice versa. Furthermore, we plot the possible states according to corresponding mean and variance in sub-periods in Figure A.1 in Appendix A.1. According to the heuristic look, the data set may have two or three states.

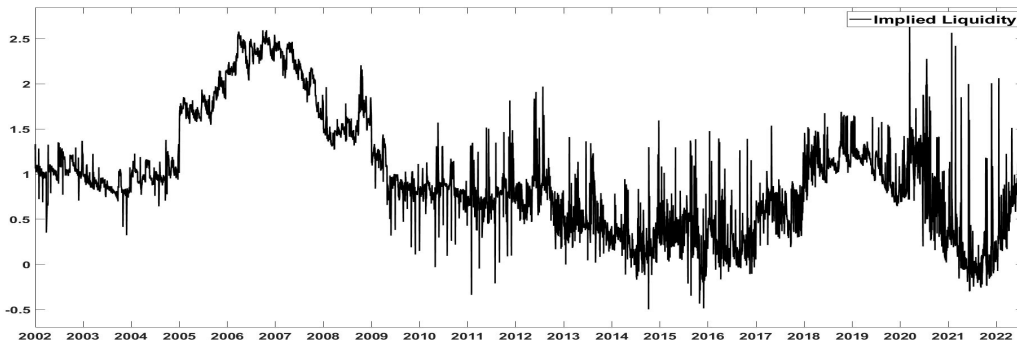


Figure 6.1: Log of implied liquidity (basis points)

## 6.2 In sample results

The initial parameters obtained through least square estimation are used as starting points of the EM algorithm. The first set of initial parameters are obtained by applying

least square estimation to the first 100 observations of the data set. The second set of initial parameters are obtained by applying least square estimation to the entire data set. Both cases assume a 1-state setting, with the entries of the generator matrix set to  $1/K$ , where  $K$  represents the number of states.

Table 6.1: Initial parameters used in empirical analysis

	1. way	2. way	3. way
$\xi_{init}$	2.077	2.8564	2.5
$\kappa_{init}$	1.29	1.92	1
$\zeta_{init}$	0.7248	0.9271	0.1

We observe that the convergence of the algorithm is achieved with different initial parameters for both 2-state and 3-state. When we assign  $1/K$  to  $a^{ij}$  for  $i \neq j$ , the algorithm cannot detect the third state. Thus, we use the following initial values in Table 6.2 for  $a^{ij}$ s.

Table 6.2: The initial values of the generator matrix

$a^{12}$	$a^{13}$	$a^{21}$	$a^{23}$	$a^{31}$	$a^{32}$
0.2	0.3	0.3	0.2	0.2	0.2

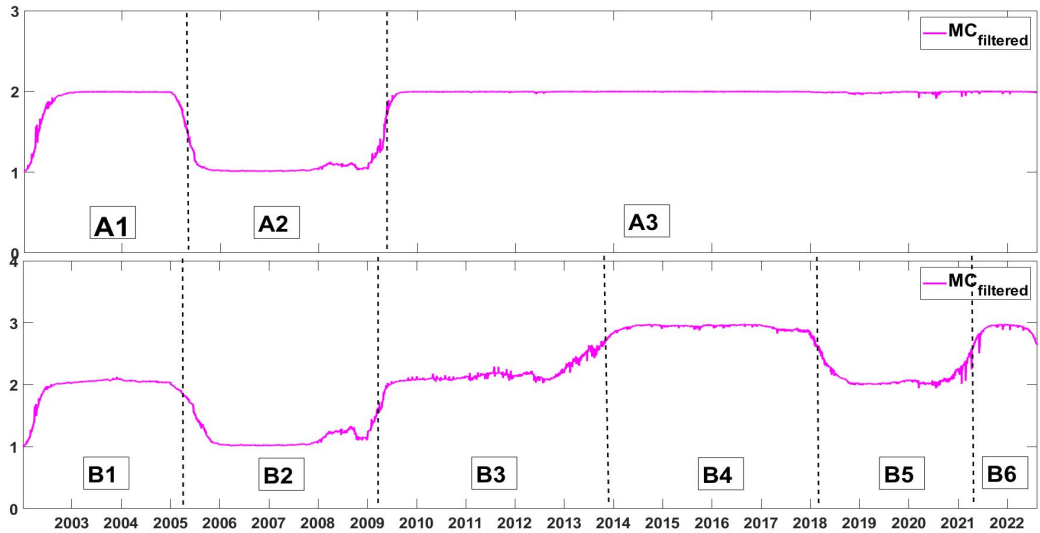


Figure 6.2: Filtered states: 2-state MC (top) and 3-state MC (bottom)

We apply the EM algorithm to the whole data set and get the following results. Although the 2- and 3-state MCs follow a similar trajectory until 2013, the 2-state MC seem not to capture the state of the underlying economic environment after then.

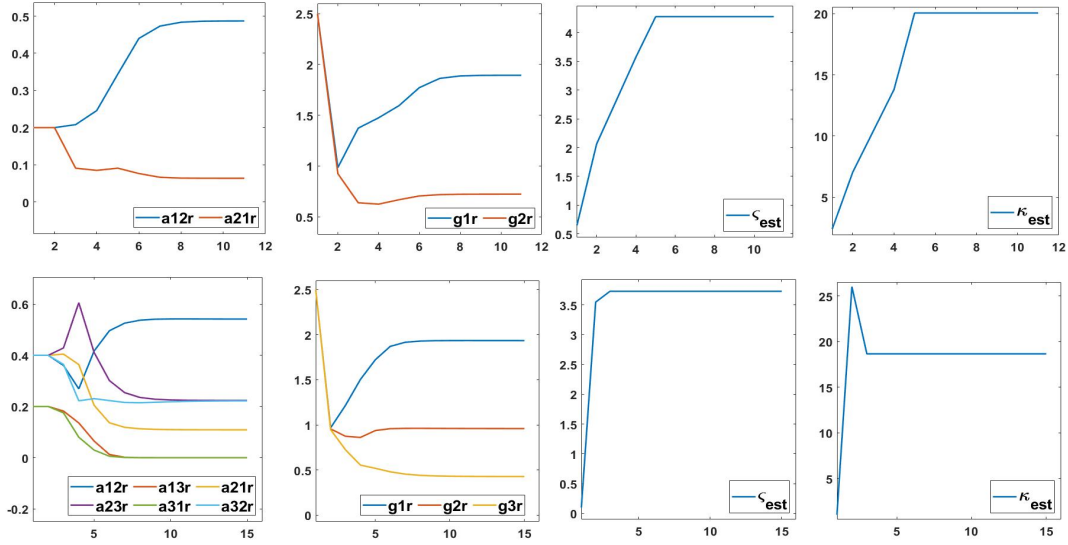


Figure 6.3: Evolution of parameter estimates for  $A$ ,  $g$ ,  $\zeta$  and  $\kappa$   
 Top: 2-state MC and bottom: 3-state MC

Table 6.3: Parameter estimates

	$\hat{a}^{12}$	$\hat{a}^{13}$	$\hat{a}^{21}$	$\hat{a}^{23}$	$\hat{a}^{31}$	$\hat{a}^{32}$
2-state MC	0.487		0.064			
3-state MC	0.542	0.000	0.109	0.222	0.000	0.222
	$\hat{g}^1$	$\hat{g}^2$	$\hat{g}^3$	$\hat{\kappa}$	$\hat{\zeta}$	
2-state MC	1.893	0.722		20.057	4.277	
3-state MC	1.934	0.959	0.428	18.658	3.727	

While 2-state model represent the 'low' and 'normal' liquidity level, 3-state model has 'low', 'intermediate' and 'high' liquidity levels.

It is natural to expect that any sound measure of market liquidity should reflect the changes in market liquidity due to changes in the underlying economic policy. It is observed in Figure 6.1 that the implied liquidity series is successful in achieving this goal. We provide the filtered trajectory of the Markov chain, representing the unknown true market liquidity level, in Figure 6.2. State transitions observed in the filtered trajectory follow the changes in the economic policy.

Naturally, the state of the market liquidity is highly dependent on the underlying monetary policy. In particular, the Federal Reserve (Fed) started cutting interest rates in 2002 in an effort to stimulate the economy following the 2001 recession. This increase in liquidity helped to spur economic growth (see region A1 (B1) of Figure



6.2).

However, by 2005, inflation was starting to become a concern and the Fed began raising interest rates in order to keep it under control. At this time, the housing market was experiencing a bubble due to the rise of subprime mortgages, and the use of complex financial instruments and leverage were on the rise, which would eventually lead to the global financial crisis of 2008, see [41, 36, 7]. The subprime mortgage market began to experience significant stress in 2007, with rising default rates and declining housing prices leading to significant losses for banks and financial institutions. The crisis continued to escalate and in response, central banks around the world, including the Fed, took several interventions such as cutting interest rates, providing liquidity support, implementing bailout and rescue packages, and implementing regulatory reforms. All these reasons led to decrease in the market liquidity level since 2005 and it experienced the lowest level between the period mid 2005 and mid 2009. The financial crisis erupted in 2007 and continued to escalate, and in response, central banks worldwide, including the Fed, took several interventions, such as cutting interest rates, providing liquidity support, implementing bailout and rescue packages, and implementing regulatory reforms. The money injections increased the liquidity level slightly in 2008 but were not enough to prevent the financial crisis. According to [7], one of the reasons of the inefficiency of the liquidity injections is that market participants were reluctant to use the discount window with the idea of not giving a bad credit signal. While the liquidity shortage during the mid-2005 and mid-2009 was not immediately reflected in the S&P 500 index, it is present in the implied liquidity series. This period is reflected in the region A2 (B2) of Figure 6.2.

By 2009, both 2- and 3-state MCs follow a trajectory accordance with the underlying economic environment. In response to the 2008 financial crisis, the implementation of a series of large-scale asset purchases, commonly referred to as quantitative easing (QE), was carried out by the Fed to decrease long-term interest rates and stimulate the economy. This led to a rapid expansion of the Fed's balance sheet, rising from \$800 billion in 2008 to \$4.5 trillion by 2014, as seen in the region (B3) of Figure 6.2. The efforts of governments and central banks to stabilize financial markets and restore economic growth changed the market structure, leading to a more liquid period, see region A3 (B3) of Figure 6.2.

In 2013, the Fed announced that it would begin to taper its asset purchases and reduce its monthly bond purchases, eventually ending its QE program in 2015. However, three QE programs carried the market high liquidity level end of 2013 and beginning of 2014. From 2014 to 2018, the Fed kept the size of its balance sheet steady, thus tapering program had limited effect on the market liquidity. Overall, the period between 2014 and 2018 was characterized by high market liquidity level, which is seen in the region (B4) of Figure 6.2.

Over the period of 2017-2018, the Fed raised interest rates several times and reduced the size of its balance sheet through a process of gradual asset runoff, which led to decrease in the market liquidity level as seen in the region (B5) of Figure 6.2. However, in response to the economic challenges posed by the COVID-19 pandemic, the Fed paused its interest rate hikes and began to expand its balance sheet again [9], which led to again high market liquidity level as seen in (B6) of Figure 6.2.

As this state of the liquidity is never seen in the past, the 2-state MC is not able to capture it. On the other hand, the 3-state MC reflects the gradually the high liquidity level in the economy.

### 6.2.1 Model selection and error analysis

The choice of the number of states for an HMM-based model can be made using a penalized likelihood approach, such as the Akaike information criterion (AIC) or Bayesian Information Criterion (BIC). This method is a standard procedure when comparing nested models, as it takes into account both the number of model parameters and the log-likelihood function of the model and applies a penalty term to models with more parameters. This method is commonly used in literature, as cited in references [53, 40, 58, 38]. The AIC is calculated using the log-likelihood function of the model, as well as the number of model parameters. Then AIC and BIC models are given respectively:

$$\text{AIC} = 2s - 2\log(\mathcal{L}(\theta))$$

$$\text{BIC} = s\log(n) - 2\log(\mathcal{L}(\theta))$$

where  $\mathcal{L}$  is the likelihood function for the model,  $N$  is the number of observations, and  $s$  denotes the number of parameters. The lower the AIC and BIC values, the better the model is considered to be among the compared the models.

To apply them, we utilize a likelihood function for the parameter set  $\theta = (a^{ij}, g^i, \varsigma, \kappa)$  given by

$$\mathcal{L}(\theta) = \prod_{n=1}^N \frac{1}{\sqrt{2\pi\hat{\varsigma}^2\Delta}} \exp\left(-\frac{((y_{n+1} - y_n - \hat{\kappa}(\langle \hat{g}, \hat{X}_n \rangle - y_n)\Delta)^2)}{2\hat{\varsigma}^2\Delta}\right).$$

Table 6.4 shows the calculated results of AIC and BIC for 2- and 3-state models. Based on the AIC and BIC results, it has been determined that the best performing model for capturing the dynamics of the market liquidity level is the 3-state model.

The one-step ahead prediction of the implied liquidity is calculated as follows

$$E[y_{n+1}|\mathcal{Y}_n] = E[y_n + \kappa(g(X_n) - y_n)\Delta + \varsigma dW_n|\mathcal{Y}_n] \quad (6.1)$$

$$\hat{y}_{n+1} = y_n + \hat{\kappa}(\hat{g}(\hat{X}_n) - y_n)\Delta \quad (6.2)$$

The parameter estimates that are used in the one-day ahead prediction can be seen in Table 6.3 and Figure 6.3. 2-state MC estimates the  $\kappa$  and  $\varsigma$  of the model higher than the 3-state MC model. State of the market liquidity cannot change from low to high or high to low since it changes gradually and needs to visit the intermediate level, namely medium level. This is also supported from 3-state MC model which gives the zero probability for the transitions between these states. One-day ahead prediction results using parameter estimates from whole data set can be seen in Figure 6.4. According to heuristic look at the figure, the predictions of 3-state model fits the actual data better than 2-state model. This result is also supported by the model selection results.

In order to evaluate the performance of the HMM-based model, the goodness of fit of the forecasts is measured using several error metrics such as the absolute mean error (MAE), mean absolute percentage error (MAPE), relative absolute error (RAE), and root mean square error (RMSE). These metrics are calculated using the observed data values  $y_n$  and the one-step ahead predictions  $\hat{y}_n$  at each time step  $n$ , as well as the sample mean  $\bar{y}$  and sample size  $N$  of the underlying process. The formulas for these

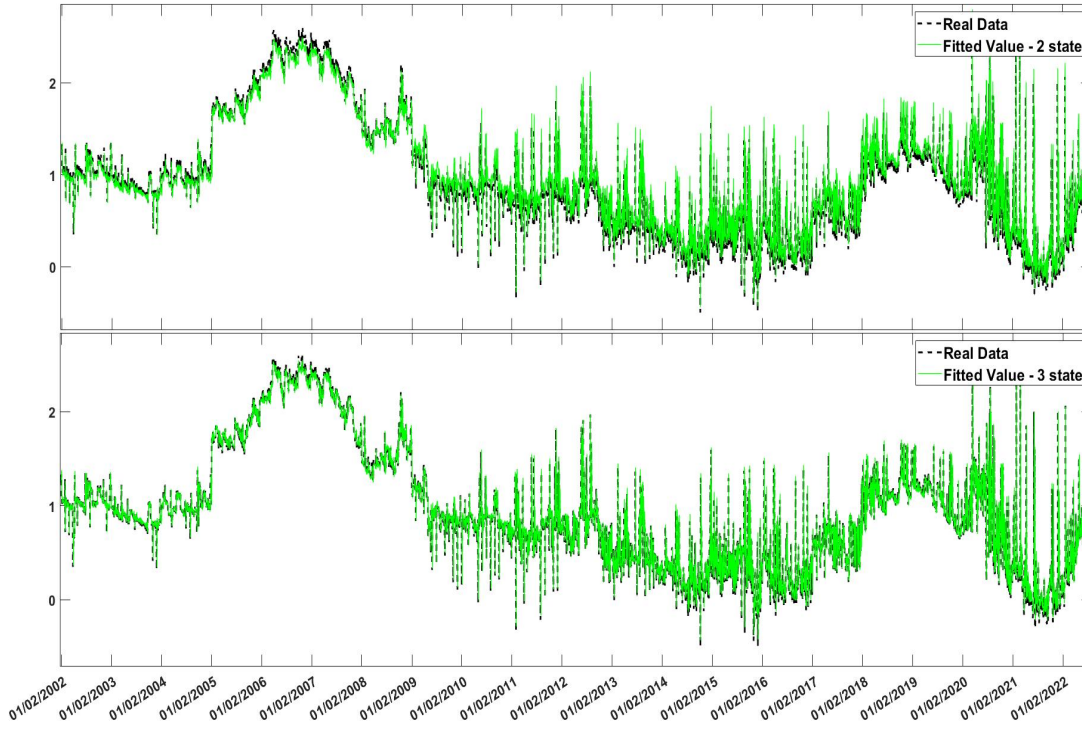


Figure 6.4: Fitted value vs real data: 2-state MC (top) and 3-state MC (bottom)

error metrics are as follows:

$$\begin{aligned}
 \text{MAE} &= \frac{1}{n} \sum_{n=1}^N |\hat{y}_n - y_n|, & \text{MAPE} &= \frac{1}{n} \sum_{n=1}^N \left| \frac{\hat{y}_n - y_n}{y_n} \right| \\
 \text{RAE} &= \frac{\sum_{n=1}^N |\hat{y}_n - y_n|}{\sum_{n=1}^N |y_n - \bar{y}|}, & \text{RMSE} &= \sqrt{\frac{1}{n} \sum_{n=1}^N (\hat{y}_n - y_n)^2}
 \end{aligned}$$

Table 6.4 shows the calculated results of goodness of fit tests. AIC and BIC for 2- and 3- state models. Based on the AIC and BIC results, it has been determined that the best performing model for capturing the dynamics of the market liquidity level is the 3-state model, which is consistent with the results of the error analysis presented in the same table.

Table 6.4: Results of error analysis - in sample results

	MAE	MAPE	RAE	RMSE	AIC	BIC
2-state MC	0.3978	2.9742e-05	0.6778	0.4556	32.9810	101.3815
3-state MC	0.1270	1.5859e-05	0.2671	0.2394	12.6006	84.8348

### 6.3 Out of sample results

We assess the effectiveness of our model in predicting market liquidity by comparing their one-day-ahead point and interval forecasts to the actual market liquidity data over the period of January 2, 2002 to June 11, 2018 to predict the period from June 16, 2018 to August 12, 2022. We use two different methods for this analysis: a static approach where we use the estimated models for the entire out-of-sample period, and a dynamic approach where we use a recursive window technique to re-estimate the parameters after each day. The estimation process in the recursive window approach starts from a fixed date and new observations are incrementally added to the estimation period, one by one.

The dynamic point forecast results of the models can be seen in the Figure 6.6. To measure the average prediction errors of the point forecasts, we calculate the MAE, MAPE, RAE and RMSE for the one-day-ahead forecasts. The results for static and dynamic approaches are given in the Table 6.5. The 3-state model outperforms the 2-state model in all measure tests for both static and recursive approaches.

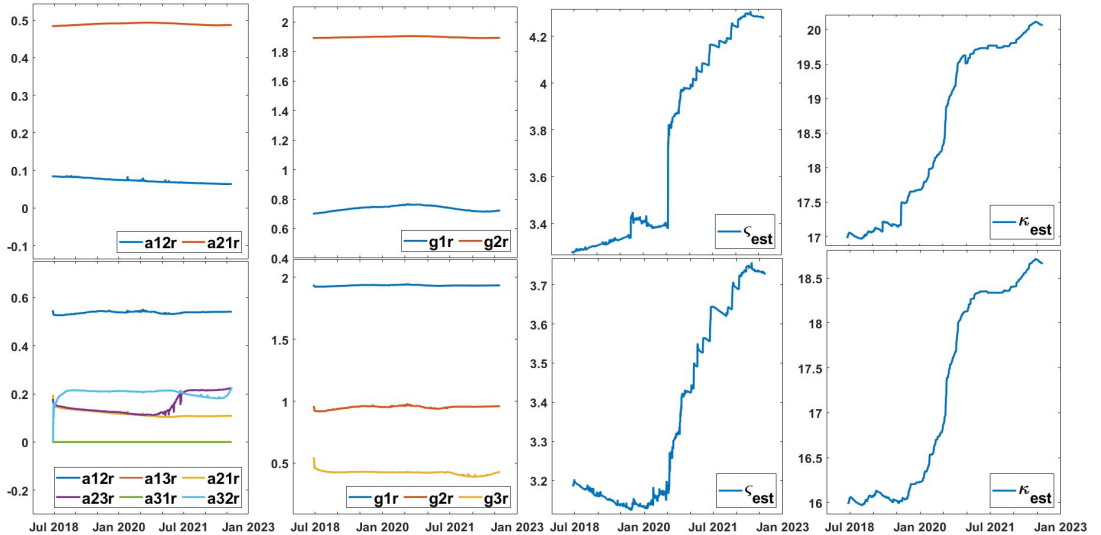


Figure 6.5: Evolution of parameter estimates for  $A$ ,  $g$ ,  $\zeta$  and  $\kappa$   
2-state MC (top) and 3-state MC (bottom)

Furthermore, we evaluate the accuracy of the models through interval forecasting. The literature provides various methods for evaluating interval forecasts, see e.g., [10, 21, 16]. Here, we use the approach proposed by [16] to generate interval forecasts

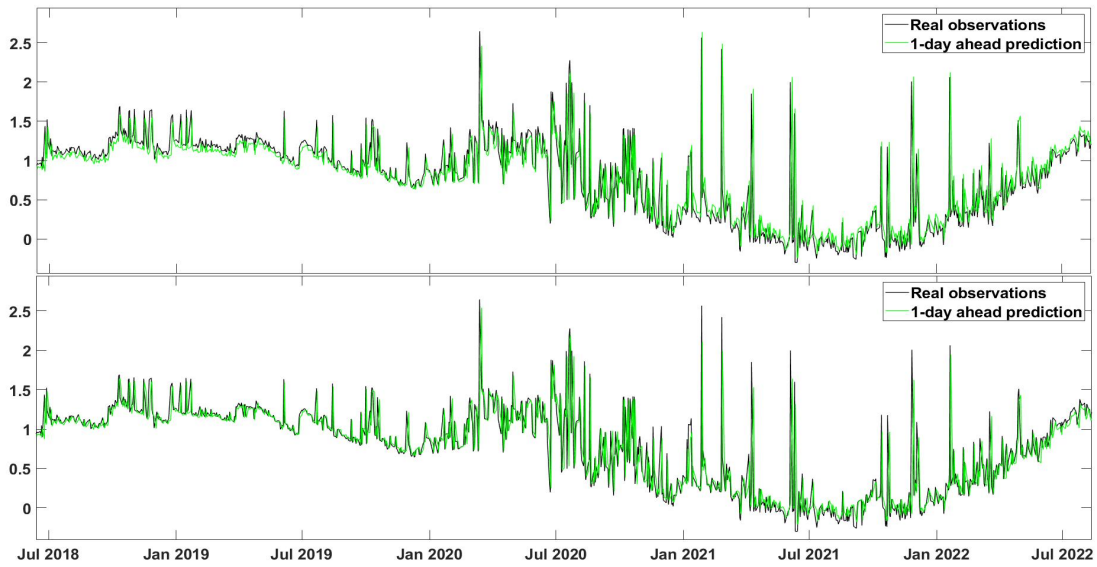


Figure 6.6: 1-day ahead prediction: 2-state MC (top) and 3-state MC (bottom)

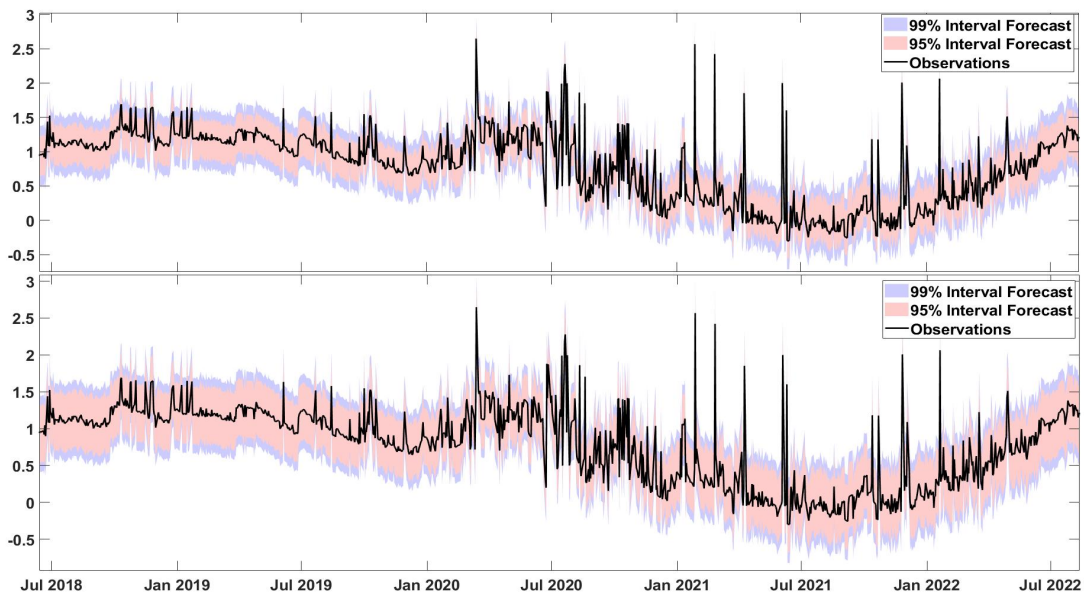


Figure 6.7: Interval forecast: 2-state MC (top) and 3-state MC (bottom)

Table 6.5: Results of error analysis - out of sample results

Static	MAE	MAPE	RAE	RMSE
2-state MC	0.6801	1.9751e-02	1.1167	0.8341
3-state MC	0.3963	1.5580e-02	0.9252	0.4417
Recursive	MAE	MAPE	RAE	RMSE
2-state MC	0.4233	1.7834e-04	0.7267	0.6479
3-state MC	0.1977	1.3588e-04	0.4253	0.3465

for our models. We set the confidence interval values at  $\alpha = 0.95$  and  $\alpha = 0.99$ , and assess the extent to which the forecasted intervals encompass the actual observations in the out-of-sample period. The results of the interval forecasts indicate that the 3-state model performs better than the 2-state model, both in the static and recursive estimation, as shown in Figures A.4 (in Appendix A.2) and 6.7, respectively. The other static forecast results can be seen in figures in Appendix A.2.





## CHAPTER 7

### CONCLUSION

In this thesis, we model the implied liquidity as a continuous-time finite state MC-modulated exponential OU process under partial information setting. The main motivation is based on the idea that any sound measure of market liquidity should reflect the policy changes, for example, from quantitative easing to tightening or financial market regime shifts from bullish to bearish market conditions. Hence, we assume that the implied liquidity series provide noisy information on the true market liquidity level, which is unobservable. To estimate the unknown parameters, we apply the EM algorithm. The E-step of the algorithm requires the derivation of finite dimensional filters for the quantities present in the filtered loglikelihood function. To this end, we first review the existing EM algorithm for the OU process and provide detailed proofs for the results. In order to avoid numerical issues and make the algorithm to function, we use filters that have a continuous dependence on the observations. The corresponding filters are known as robust filters. Instead of directly discretizing continuous time filters, we discretize the robust filters. This approach provides a discrete time setting however it has an explicit approximation of the continuous time filters. This helps us to work under the discrete time setting and also enable us to obtain the variance estimate of the model within the EM algorithm.

We evaluate the performance of the algorithm and compare it to existing alternatives in the literature using an extensive simulation study. The performance evaluation is based on the sensitivity to changes in step size, drift, and volatility parameters. According to results, the robust filters outperformed the alternatives.

In our empirical analysis, we analyze both in-sample and out-of-sample test results

using statistical metrics, and find that the three-regime model performs better than the two-regime model in capturing the economic dynamics that explain the market liquidity level in financial markets.

We put forward and empirically tested a new way of estimating and predicting liquidity levels in the financial markets. This approach provides a quantitative methodology that supports economic interpretation of the liquidity proxy. Knowing true market liquidity levels can be useful for market participants. The proposed modeling and estimation set up can be effectively exploited for different financial assets that follow mean reverting process. Based on our results, we suggest that further analysis of data with different frequencies should be carried out to gain insights about liquidity risk over different time periods, potentially involving the inclusion of new drivers, factors, and determinants of liquidity in the filtering experiments. This may require the tweaking of the HMM-driven OU process to accommodate new inputs leading to new filters. Also, long term prediction can be applied in the future work.

## REFERENCES

- [1] H. Albrecher, F. Guillaume, and W. Schoutens, Implied liquidity: Model sensitivity, *Journal of Empirical Finance*, 23, pp. 48–67, 2013.
- [2] Y. Amihud, Illiquidity and stock returns: cross-section and time-series effects, *Journal of Financial Markets*, 5(1), pp. 31–56, 2002.
- [3] P. Artzner, F. Delbaen, J.-M. Eber, and D. Heath, Coherent measures of risk, *Mathematical Finance*, 9(3), pp. 203–228, 1999.
- [4] G. Barles and H. M. Soner, Option pricing with transaction costs and a nonlinear black-scholes equation., *Finance & Stochastics*, 2(4), 1998.
- [5] A. Beber and M. Pagano, Measuring liquidity in the tlx market, University of Naples Federico II, 2008.
- [6] A. D. Brunner, Using measures of expectations to identify the effects of a monetary policy shock, 1996.
- [7] M. K. Brunnermeier, Deciphering the liquidity and credit crunch 2007-2008, *Journal of Economic Perspectives*, 23(1), pp. 77–100, 2009.
- [8] M. K. Brunnermeier and L. H. Pedersen, Market liquidity and funding liquidity, *The Review of Financial Studies*, 22(6), pp. 2201–2238, 2009.
- [9] A. Chari, K. Dilts Stedman, and C. Lundblad, Taper tantrums: Quantitative easing, its aftermath, and emerging market capital flows, *The Review of Financial Studies*, 34(3), pp. 1445–1508, 2021.
- [10] C. Chatfield, Calculating interval forecasts, *Journal of Business & Economic Statistics*, 11(2), pp. 121–135, 1993.
- [11] L. Chen, L. Shen, and Z. Zhou, Understand funding liquidity and market liquidity in a regime-switching model, *International Journal of Finance & Economics*, pp. 1–17, 2021.
- [12] A. Cherny and D. Madan, New measures for performance evaluation, *The Review of Financial Studies*, 22(7), pp. 2571–2606, 2009.
- [13] J. Y. Choi, D. Salandro, and K. Shastri, On the estimation of bid-ask spreads: Theory and evidence, *Journal of Financial and Quantitative Analysis*, 23(2), pp. 219–230, 1988.

- [14] T. Chordia, R. Roll, and A. Subrahmanyam, Market liquidity and trading activity, *The Journal of Finance*, 56(2), pp. 501–530, 2001.
- [15] T. Chordia, A. Sarkar, and A. Subrahmanyam, An empirical analysis of stock and bond market liquidity, *The Review of Financial Studies*, 18(1), pp. 85–129, 2005.
- [16] P. F. Christoffersen, Evaluating interval forecasts, *International Economic Review*, pp. 841–862, 1998.
- [17] J. Clark, The design of robust approximations to the stochastic differential equations of nonlinear filtering, *Communication Systems and Random Process Theory*, 25, pp. 721–734, 1978.
- [18] J. M. Clark and R. Cameron, The maximum rate of convergence of discrete approximations for stochastic differential equations, in *Stochastic differential systems filtering and control*, pp. 162–171, Springer, 1980.
- [19] S. N. Cohen and R. J. Elliott, *Stochastic calculus and applications*, volume 2, Springer, 2015.
- [20] J. M. Corcuera, F. Guillaume, D. B. Madan, and W. Schoutens, Implied liquidity: towards stochastic liquidity modelling and liquidity trading, *International Journal of Portfolio Analysis and Management*, 1(1), pp. 80–91, 2012.
- [21] C. Crnkovic and J. Drachman, A universal tool to discriminate among risk measurement techniques, *Risk*, 12, pp. 74–83, 1995.
- [22] J. Cvitanić and I. Karatzas, Hedging and portfolio optimization under transaction costs: A martingale approach 1 2, *Mathematical Finance*, 6(2), pp. 133–165, 1996.
- [23] V. T. Datar, N. Y. Naik, and R. Radcliffe, Liquidity and stock returns: An alternative test, *Journal of Financial Markets*, 1(2), pp. 203–219, 1998.
- [24] M. H. Davis, V. G. Panas, and T. Zariphopoulou, European option pricing with transaction costs, *SIAM Journal on Control and Optimization*, 31(2), pp. 470–493, 1993.
- [25] H. Demsetz, The cost of transacting, *The Quarterly Journal of Economics*, 82(1), pp. 33–53, 1968.
- [26] A. Díaz and A. Escribano, Measuring the multi-faceted dimension of liquidity in financial markets: A literature review, *Research in International Business and Finance*, 51, p. 101079, 2020.
- [27] D. Easley and M. O’Hara, Adverse selection and large trade volume: The implications for market efficiency, *Journal of Financial and Quantitative Analysis*, 27(2), pp. 185–208, 1992.

- [28] R. J. Elliott, P. Fischer, and E. Platen, Filtering and parameter estimation for a mean reverting interest rate model, *Canadian Applied Mathematics Quarterly*, 7(4), pp. 381–400, 1999.
- [29] R. J. Elliott and V. Krishnamurthy, New finite-dimensional filters for parameter estimation of discrete-time linear gaussian models, *IEEE Transactions on Automatic Control*, 44(5), pp. 938–951, 1999.
- [30] R. F. Engle III and J. Lange, Measuring, forecasting and explaining time varying liquidity in the stock market, National Bureau of Economic Research, 1997.
- [31] M. J. Fleming, Measuring treasury market liquidity, FRB of New York Staff Report, (133), 2001.
- [32] M. D. Flood, J. Liechty, and T. Piontek, Systemwide commonalities in market liquidity, Available at SSRN 2612348, 2015.
- [33] C. Florackis, A. Gregoriou, and A. Kostakis, Trading frequency and asset pricing on the london stock exchange: Evidence from a new price impact ratio, *Journal of Banking & Finance*, 35(12), pp. 3335–3350, 2011.
- [34] T. Foucault, M. Pagano, A. Roell, and A. Röell, *Market liquidity: theory, evidence, and policy*, Oxford University Press, 2013.
- [35] A. Gabrielsen, M. Marzo, and P. Zagaglia, Measuring market liquidity: An introductory survey, arXiv preprint arXiv:1112.6169, 2011.
- [36] G. Gorton, *Misunderstanding financial crises: Why we don't see them coming*, Oxford University Press, 2012.
- [37] R. Y. Goyenko, C. W. Holden, and C. A. Trzcinka, Do liquidity measures measure liquidity?, *Journal of Financial Economics*, 92(2), pp. 153–181, 2009.
- [38] X. Gu, R. Mamon, M. Davison, and H. Yu, An automated financial indices-processing scheme for classifying market liquidity regimes, *International Journal of Control*, 94(3), pp. 735–756, 2021.
- [39] F. Guillaume, G. Junike, P. Leoni, and W. Schoutens, Implied liquidity risk premia in option markets, *Annals of Finance*, 15, pp. 233–246, 2019.
- [40] M. R. Hardy, A regime-switching model of long-term stock returns, *North American Actuarial Journal*, 5(2), pp. 41–53, 2001.
- [41] E. Helleiner, Understanding the 2007–2008 global financial crisis: Lessons for scholars of international political economy, *Annual Review of Political Science*, 14, pp. 67–87, 2011.
- [42] M. R. James, V. Krishnamurthy, and F. Le Gland, Time discretization of continuous-time filters and smoothers for hmm parameter estimation, *IEEE Transactions on Information Theory*, 42(2), pp. 593–605, 1996.

- [43] J. M. Keynes, *Treatise on money: Pure theory of money vol. i*, 1930.
- [44] M. Leippold and S. Schärer, Discrete-time option pricing with stochastic liquidity, *Journal of Banking & Finance*, 75, pp. 1–16, 2017.
- [45] X. Lou and T. Shu, Price impact or trading volume: Why is the amihud (2002) measure priced?, *The Review of Financial Studies*, 30(12), pp. 4481–4520, 2017.
- [46] D. Madan and W. Schoutens, *Applied conic finance*, Cambridge University Press, 2016.
- [47] D. B. Madan and A. Cherny, Markets as a counterparty: an introduction to conic finance, *International Journal of Theoretical and Applied Finance*, 13(08), pp. 1149–1177, 2010.
- [48] D. Nguyen, S. Mishra, A. Prakash, and D. K. Ghosh, Liquidity and asset pricing under the three-moment capm paradigm, *Journal of Financial Research*, 30(3), pp. 379–398, 2007.
- [49] O. Oesterhelweg and D. Schiereck, Measuring concept for the liquidity of financial markets, *Die Bank*, 33, pp. 390–397, 1993.
- [50] L. H. Pedersen, *When everyone runs for the exit*, 2009.
- [51] P. Protter, *Stochastic Integration and Differential Equations. A new Approach*, volume 21, *Appl. Math. (New York)*, 1990.
- [52] R. Roll, A simple implicit measure of the effective bid-ask spread in an efficient market, *The Journal of Finance*, 39(4), pp. 1127–1139, 1984.
- [53] T. Rydén, T. Teräsvirta, and S. Åsbrink, Stylized facts of daily return series and the hidden markov model, *Journal of Applied Econometrics*, 13(3), pp. 217–244, 1998.
- [54] A. Sarr and T. Lybek, Measuring liquidity in financial markets, Available at SSRN 880932, 2002.
- [55] E. S. Schwartz, The stochastic behavior of commodity prices: Implications for valuation and hedging, *The Journal of Finance*, 52(3), pp. 923–973, 1997.
- [56] P. Shen and R. M. Starr, Market-makers’ supply and pricing of financial market liquidity, *Economics Letters*, 76(1), pp. 53–58, 2002.
- [57] S. E. Shreve and H. M. Soner, Optimal investment and consumption with transaction costs, *The Annals of Applied Probability*, pp. 609–692, 1994.
- [58] A. Tenyakov, R. Mamon, and M. Davison, Filtering of a discrete-time hmm-driven multivariate ornstein-uhlenbeck model with application to forecasting market liquidity regimes, *IEEE Journal of Selected Topics in Signal Processing*, 10(6), pp. 994–1005, 2016.

[59] G. E. Uhlenbeck and L. S. Ornstein, On the theory of the brownian motion, Physical Review, 36(5), p. 823, 1930.





# APPENDIX A

## APPENDICES

### A.1 Possible states in the data

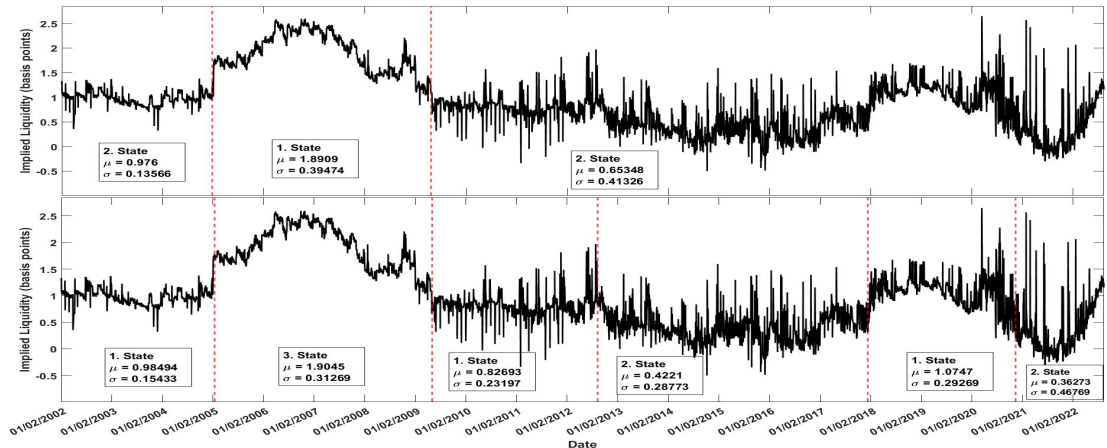


Figure A.1: Possible states in the data

### A.2 Results of static out of sample test

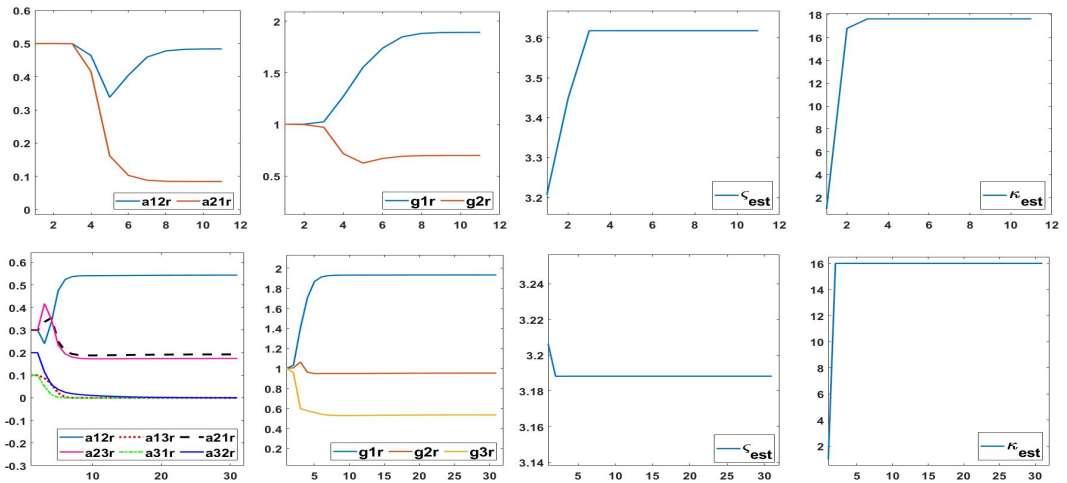


Figure A.2: Evolution of parameter estimates for  $A$ ,  $g$ ,  $\zeta$  and  $\kappa$   
2-state MC (top) and 3-state MC (bottom)

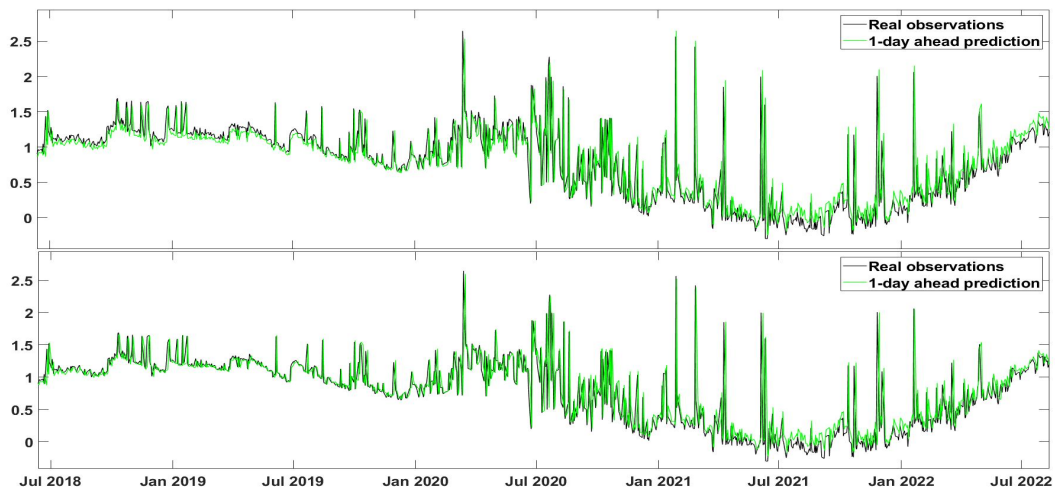


Figure A.3: 1-day ahead prediction: 2-state MC (top) and 3-state MC (bottom)

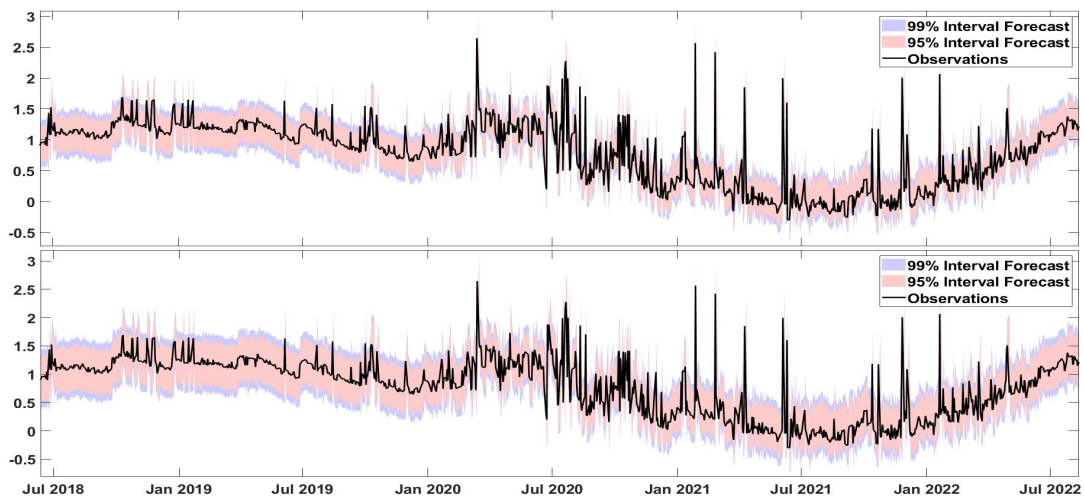


Figure A.4: Interval forecast: 2-state MC (top) and 3-state MC (bottom)

# CURRICULUM VITAE

## PERSONAL INFORMATION

**Surname, Name:** Yerli, Cigdem

**Nationality:** Turkish (TC)

## EDUCATION

<b>Degree</b>	<b>Institution</b>	<b>Year of Graduation</b>
PhD.	Financial Mathematics, IAM, METU, Turkiye	2023
M.S.	Finance and Investment, Business School, Durham University, UK	2013
B.S.	Business Administration, Cankaya University, Turkiye	2011

## PROFESSIONAL EXPERIENCE

<b>Year</b>	<b>Place</b>	<b>Enrollment</b>
2015 -	Bartın Vocational School/Bartın University	Lecturer

## PUBLICATIONS

- YERLİ, C., & KESTEL, S. (2022). Risk Distribution Among Uncorrelated Risk Factors: Diversified Risk Parity. Hacettepe Üniversitesi İktisadi ve İdari Bilimler Fakültesi Dergisi, 40(2), 419-439.

- YERLİ, C., & EKSI-ALTAY, Z. and KESTEL, S. (2023). The On the information content of implied liquidity measure: Evidence from S&P 500 index options. *It has been submitted to Finance Research Letters.*

## **AWARDS**

- TUBITAK 2214-A, Visting the Institute for Statistics and Mathematics at WU from 04.2022 to 04.2023, Vienna, Austria.
- YLSY 2011, M.Sc, in Finance and Investment, Durham Business School, Durham, UK.